Tel1/ATM Signaling to the Checkpoint Contributes to Replicative Senescence in the Absence of Telomerase

Luca Menin,[1] Chiara Vittoria Colombo, Giorgia Maestrini, Maria Pia Longhese,[2] and Michela Clerici[2]
Dipartimento di Biotecnologie e Bioscienze, Università di Milano–Bicocca, Milano 20126, Italy
ORCID IDs: 0000-0003-1726-2034 (M.P.L.); 0000-0001-9152-0156 (M.C.)

ABSTRACT Telomeres progressively shorten at every round of DNA replication in the absence of telomerase. When they become critically short, telomeres trigger replicative senescence by activating a DNA damage response that is governed by the Mec1/ATR and Tel1/ATM protein kinases. While Mec1/ATR is known to block cell division when extended single-stranded DNA (ssDNA) accumulates at eroded telomeres, the molecular mechanism by which Tel1/ATM promotes senescence is still unclear. By characterizing a Tel1–hy184 mutant variant that compensates for the lack of Mec1 functions, we provide evidence that Tel1 promotes senescence by signaling to a Rad9-dependent checkpoint. Tel1–hy184 anticipates senescence onset in telomerase-negative cells, while the lack of Tel1 or the expression of a kinase-defective (kd) Tel1 variant delays it. Both Tel1–hy184 and Tel1–kd do not alter ssDNA generation at telomeric DNA ends. Furthermore, Rad9 and (only partially) Mec1 are responsible for the precocious senescence promoted by Tel1–hy184. This precocious senescence is mainly caused by the F1751I, D1985N, and E2133K amino acid substitutions, which are located in the FRAP–ATM–TRAPP domain of Tel1 and also increase Tel1 binding to DNA ends. Altogether, these results indicate that Tel1 induces replicative senescence by directly signaling dysfunctional telomeres to the checkpoint machinery.

KEYWORDS Tel1; telomere; replicative senescence; checkpoint

TELOMERES are nucleoprotein structures that cap the ends of linear chromosomes. In most eukaryotes, telomeric DNA comprises a variable number of repetitive TG-rich sequences oriented in the 5′→3′ direction that terminate with a 3′ protruding single-stranded DNA (ssDNA) end (G-tail) (Wellinger and Zakian 2012; de Lange 2018). Telomeres are coated by a specific set of proteins that shield them from DNA double-strand break (DSB) signaling and repair activities, which could otherwise cause chromosome rearrangements (Maciejowski and de Lange 2017). This protective function is achieved by the shelterin complex in vertebrates (TRF1, TRF2, POT1, TPP1, TIN2, and Rap1) (de Lange 2018), and by the Rap1, Rif1, Rif2, Sir2, Sir3, and Sir4 proteins in *Saccharomyces cerevisiae* (Wellinger and Zakian 2012). In all eukaryotes, a second chromosome-end capping pathway exists, which involves a complex named CST (Cdc13–Stn1–Ten1 in budding yeast) (Giraud–Panis *et al.* 2010).

The addition of telomeric repeats depends on the action of telomerase, a ribonucleoprotein complex with a reverse transcriptase subunit (TR or TERT in mammalian cells, and Est2 in budding yeast) that extends the TG-rich strand of chromosome ends by using an associated noncoding RNA (TERC in mammals; *TLC1* in *S. cerevisiae*) as a template (Armstrong and Tomita 2017; Vasianovich and Wellinger 2017). The DNA polymerase α–primase complex accomplishes the fill-in synthesis of the complementary CA-rich strand (Grossi *et al.* 2004).

Telomerase components are expressed in dividing cells, such as germ and stem cells, and in unicellular eukaryotes, while their expression is downregulated in most human somatic cells (Kim *et al.* 1994; Mozdy and Cech 2006). These telomerase-deficient cells experience progressive telomere shortening at each round of DNA replication, which leads to an irreversible cell division arrest known as replicative senescence (Hayflick 1965; Lundblad and Szostak 1989; Harley *et al.* 1990; Stewart and Weinberg 2006; Teixeira

doi: https://doi.org/10.1534/genetics.119.302391
Manuscript received March 7, 2019; accepted for publication July 27, 2019; published Early Online August 7, 2019.
Supplemental material available at FigShare: https://doi.org/10.25386/genetics.8980337.
[1]Present address: IFOM (Fondazione Istituto FIRC di Oncologia Molecolare), Via Adamello 16, Milano 20139, Italy.
[2]Corresponding authors: Dipartimento di Biotecnologie e Bioscienze, Università di Milano–Bicocca, Piazza della Scienza 2, Milano 20126, Italy. E-mails: mariapia.longhese@unimib.it; michela.clerici@unimib.it

2013; Shay 2016). Therefore, telomeres are considered molecular clocks that limit cell replicative life span, thus acting as a potent tumor-suppressive mechanism. Consistently, most tumor cells express telomerase, which confers them infinite replicative potential (Stewart and Weinberg 2006; Shay 2016; Maciejowski and de Lange 2017).

Telomere shortening causes a progressive loss of the protective structures at chromosome ends, which are then exposed to DSB recognition factors, whose activation triggers a checkpoint response that inhibits cell cycle progression (Enomoto *et al.* 2002; d'Adda di Fagagna *et al.* 2003; IJpma and Greider 2003; Grandin *et al.* 2005; Teixeira 2013). The *S. cerevisiae* protein kinases Tel1 and Mec1, as well as their respective human counterparts ATM and ATR, are the master regulators of the DSB response. Tel1/ATM is activated by blunt or minimally processed DNA ends, where it is recruited through the interaction with the MRX (Mre11–Rad50–Xrs2)/MRN (Mre11–Rad50–Nbs1) complex, while Mec1/ATR and its interactor Ddc2/ATRIP primarily recognize ssDNA stretches coated by the Replication Protein A complex (Shiloh and Ziv 2013; Villa *et al.* 2016). Once activated, Tel1/ATM and Mec1/ATR block the cell cycle trough phosphorylation of the effector kinases Rad53/Chk2 and Chk1, whose activation requires Rad9/53BP1 and Mrc1/Claspin adaptors (Moriel-Carretero *et al.* 2019).

Moreover, MRX-dependent association of Tel1 to short telomeres induces their telomerase-dependent elongation (Ritchie *et al.* 1999; Ritchie and Petes 2000; Tsukamoto *et al.* 2001; Arnerić and Lingner 2007; Hector *et al.* 2007; Sabourin *et al.* 2007). Tel1/ATM promotes the nucleolytic degradation of the 5′ DNA ends by the MRX/MRN complex at both telomeres and DSBs (Mantiero *et al.* 2007; Martina *et al.* 2012). Degradation of the 5′ CA-rich strand at telomeres generates transient 3′ TG-rich overhangs that recruit telomerase (Wellinger *et al.* 1996; Teixeira *et al.* 2004; Goudsouzian *et al.* 2006; Bianchi and Shore 2007; Fallet *et al.* 2014), while DSB-end processing creates 3′-ended ssDNA tails that trigger both DSB repair by homologous recombination and activation of a Mec1-dependent checkpoint (Villa *et al.* 2016).

Telomerase removal in yeast causes progressive telomere shortening as well as the activation of a Mec1-dependent checkpoint that induces senescence (Enomoto *et al.* 2002; IJpma and Greider 2003; Grandin *et al.* 2005). Furthermore, the lack of telomere-processing proteins, such as any MRX component, delays senescence, while the absence of processing inhibitors such as Rif2, anticipates it, indicating that ssDNA is one of the signals that trigger senescence (Abdallah *et al.* 2009; Khadaroo *et al.* 2009; Ballew and Lundblad 2013). The lack of Tel1 also delays senescence (Ritchie *et al.* 1999; Enomoto *et al.* 2002; Abdallah *et al.* 2009; Gao *et al.* 2010; Chang and Rothstein 2011; Ballew and Lundblad 2013). As Tel1 promotes ssDNA generation at both DSBs and telomeres (Mantiero *et al.* 2007; Martina *et al.* 2012), the delayed senescence in Tel1-deficient cells has been proposed to be due to a reduced amount of ssDNA at telomeres (Gao *et al.* 2010; Ballew and Lundblad 2013; Fallet *et al.* 2014).

Here, we studied the function of Tel1 in senescence by using both a hyperactive Tel1–hy184 mutant variant, which has been identified because of its ability to compensate for the lack of Mec1 functions (Baldo *et al.* 2008), and a kinase-defective (kd) Tel1–kd variant (Mallory and Petes 2000). We showed that, in telomerase-deficient cells, Tel1–hy184 anticipates the onset of senescence compared to wild-type Tel1, while both Tel1–kd and the lack of Tel1 delay senescence. Strikingly, neither Tel1–hy184 nor Tel1–kd affects the generation of ssDNA at telomeres, indicating that Tel1's function in promoting senescence is not directly linked to its function in telomere processing. Furthermore, the anticipated senescence triggered by Tel1–hy184 completely depends on Rad9 and only partially on Mec1, indicating that Tel1 promotes senescence mainly by directly signaling the presence of dysfunctional telomeres to a Rad9-dependent checkpoint.

Materials and Methods

Yeast strains and media

S. cerevisiae strains used in this work are listed in Supplemental Material, Table S1 and are isogenic to W303 (*MAT***a**/α *ade2–1 can1–100 his3–11,15 leu2–3,112 trp1–1 ura3–1 rad5–535*) or UCC5913 (*MAT***a***–inc ade2–101 lys2–801 his3–*Δ*200 trp1–*Δ*63 ura3–52 leu2–*Δ*1::GAL1–HO–LEU2 VII–L::ADE2–TG(1–3)–HO site–LYS2*), kindly provided by D. Gottschling (Fred Hutchinson Cancer Research Center, Seattle). A yeast strain carrying the *sgs1–D664*Δ allele was kindly provided by R. Rothstein (Columbia University, New York City, NY).

All genetic manipulations were verified by polymerase chain reaction (PCR) and/or Southern blot analyses. Gene deletions were carried out by one-step PCR methods. Cells were grown in YEP medium (1% yeast extract and 2% peptone) supplemented with 2% glucose (YEPD), 2% raffinose, or 2% raffinose and 3% galactose (YEPRG).

Senescence assay

Senescence analysis was performed by serial passages in liquid YEPD medium of spore clones obtained from heterozygous diploids carrying the deletion of either the *EST2* or *TLC1* gene, and the mutation of interest, thus ensuring that all the strains inherited telomeres of similar length and from the same epigenetic environment. After sporulation, meiotic tetrads were dissected on YEPD plates that were incubated at 30°, followed by spore genotyping. Next, 48 hr after tetrad dissection, haploid spore clones with the desired genotypes were recultured directly from the microdissection plates into liquid YEPD medium at concentrations of 5×10^4 cells/ml and grown at 30°. Every 24 hr, cell density was determined and cell cultures were diluted back to 5×10^4 cells/ml in YEPD. The mean cell concentration of at least four independent spores with the same genotype against the number of

generations [population doubling (PD)] was plotted on a graph to visualize the senescence kinetics. As we estimated that colonies on the microdissection plates were grown for ~20 PDs when they were inoculated in liquid medium and that an additional 10 PDs occurred in liquid medium before the first cell density measurement, the starting point in the senescence assays was set to 30 PDs.

Southern blot analysis of telomere length

Yeast genomic DNA prepared via standard methods was digested with *Xho*I restriction enzyme. The resulting DNA fragments were separated by agarose gel electrophoresis in TBE 1× buffer in a 0.8% agarose gel. DNA was blotted onto a GeneScreen nylon membrane (New England Nuclear, Boston, MA). Hybridization was carried out at 50° with a ^{32}P-labeled poly(GT) probe obtained by random priming (DECAprimeTM kit by Ambion).

In-gel hybridization for the analysis of the G-tail

Yeast genomic DNA was purified with a genomic-tip 100/G extraction kit purchased from QIAGEN (Valencia, CA). Visualization of the single-stranded overhangs at native telomeres was performed by in-gel hybridization as previously described (Dionne and Wellinger 1996). The same gel was denatured and hybridized with the same end-labeled CA-rich oligonucleotide as a loading control.

Analysis of ssDNA generation at an artificial telomere induced by a cut with the HOmothallic switching endonuclease (HO) telomere

81-bp TG repeats adjacent to a recognition sequence for the HO endonuclease were placed at the ADH4 locus on chromosome VII in UCC5913 and derivative strains, which express the *HO* gene from a galactose-inducible *GAL1* promoter. *Rsa*I- and *Eco*RV-digested genomic DNA was subjected to denaturing polyacrylamide gel electrophoresis, and transferred onto a positively charged nylon membrane. The filter was then hybridized with a single-stranded RNA probe complementary to the 5′ CA-strand to a site located 212 nt centromere-proximal to the HO-cutting site. The ssRNA probe was obtained by *in vitro* transcription using Promega (Madison, WI) Riboprobe System-T7 and a pGEM-7Zf-based plasmid as a template. For quantitative analysis of the CA-strand signals, the ratio between the intensities of the cut CA-strands and loading control bands was calculated by using the National Institutes of Health ImageJ program.

Chromatin immunoprecipitation

Chromatin immunoprecipitation (ChIP) assays were performed as previously described (Martina *et al.* 2012). Data are expressed as fold enrichment at the HO-induced short telomere or at the VI-R native telomere over that at the noncleaved *ARO1* locus, after normalization of each ChIP signal to the corresponding amount of immunoprecipitated protein and input for each time point. Fold enrichment was then normalized to the efficiency of DSB induction. Primers are listed in Table S2.

Immunoprecipitation and kinase assays

Immunoprecipitation and kinase assays were performed as previously described (Baldo *et al.* 2008). Protein extracts were incubated for 2 hr at 4° with 75 μl of a 50% (v/v) protein A–Sepharose resin covalently linked to anti-HA monoclonal antibodies (12CA5). Kinase reactions were incubated at 30° for 30 min. Sodium dodecyl sulfate (SDS) gel-loading buffer was added to the samples and bound proteins were resolved by SDS-18% polyacrylamide gel electrophoresis, and visualized after exposure of the gels to autoradiography films. The residual 300 μl of each resuspended resin were dried, resuspended in 10 μl of loading buffer, boiled, and subjected to western blot analysis with anti-HA antibodies.

Quantitative amplification of ssDNA

Yeast genomic DNA was purified with agenomic-tip 100/G extraction kit purchased from QIAGEN, and subtelomeric ssDNA was quantified according to Booth *et al.* (2001) and Zubko *et al.* (2006) using primers listed in Table S2.

Other techniques

Flow cytometric analyses of DNA content were performed on a Becton Dickinson FACScan. Rad53 was detected by using anti-Rad53 polyclonal antibodies kindly provided by J. Diffley (The Francis Crick Institute, London, UK). For drop-test assays, the concentrations of exponentially growing overnight cultures were determined, and 10-fold serial dilutions of equivalent cell numbers were spotted out onto plates containing the indicated medium. Images were captured after 2–3 days of growth at 30°. For cell viability assays, the same numbers of cells were plated onto YEPD plates with or without different concentrations of hydroxyurea (HU). Colony-forming units were determined after 2–3 days of growth at 30°.

Data availability

Table S1 includes the names and genotypes of all strains used in this work. Table S2 includes sequences of primers used for ChIP and quantitative amplification of ssDNA (QAOS) assays. Figure S1 illustrates the viability of *est2*Δ and *est2*Δ *TEL1–hy184* cells during a senescence assay. Figure S2 shows that Tel1–hy184 promotes precocious senescence in *tlc1*Δ cells. Figure S3 shows that *est2*Δ cells accumulate ssDNA at telomeres and that *TEL1–hy184* does not increase the lethality of *cdc13–1* cells. Figure S4 illustrates the kinetics of senescence and Rad53 phosphorylation, in *est2*Δ and *est2*Δ *TEL1–hy184* cells lacking Rad9 or Mec1. All the strains are available upon request. All data necessary for confirming the conclusions of the article are present within the article and the associated supplemental files. Supplemental material available at FigShare: https://doi.org/10.25386/genetics.8980337.

Results

The tel1Δ and TEL1–hy184 alleles exert opposite effects on replicative senescence onset in telomerase-negative cells

Tel1 is recruited to short telomeres in telomerase-deficient cells (Sabourin *et al.* 2007; Abdallah *et al.* 2009) and promotes replicative senescence by an unknown mechanism (Ritchie *et al.* 1999; Enomoto *et al.* 2002; Abdallah *et al.* 2009; Gao *et al.* 2010; Chang and Rothstein 2011; Ballew and Lundblad 2013).

We investigated the function of Tel1 in promoting replicative senescence by taking advantage of hyperactive *TEL1–hy* mutant alleles that partially relieve both the hypersensitivity to genotoxic agents and the checkpoint defects of cells lacking the checkpoint kinase Mec1 (Baldo *et al.* 2008). We focused on the Tel1–hy184 mutant variant, which carries the F1752I, D1985N, E2133K, R2735G, and E2737V amino acid substitutions. This mutant variant, which only slightly increases telomere length, and possesses an intrinsic kinase activity similar to or slightly higher than wild-type Tel1, restores Rad53 phosphorylation and cell cycle arrest in *mec1Δ* cells more efficiently than other Tel1–hy variants (Baldo *et al.* 2008). In particular, *TEL1–hy184 mec1Δ* cells showed almost wild-type levels of Rad53 phosphorylation after both UV irradiation and treatment with bleomycin, although Rad53 phosphorylation was delayed compared to *MEC1* cells (Baldo *et al.* 2008). *TEL1–hy184* also increased the resistance of *mec1Δ* cells to low doses of the replication inhibitor HU (Baldo *et al.* 2008; Figure S1A).

The effect of *TEL1–hy184* and *tel1Δ* alleles on the proliferative decline in cells lacking the Est2 telomerase subunit was assayed by performing standard senescence assays in liquid medium. In liquid rich medium at 30°, we inoculated multiple wild-type, *tel1Δ*, *TEL1–hy184*, *est2Δ*, *est2Δ tel1Δ*, and *est2Δ TEL1–hy184* spore clones derived from the meiotic products of *EST2/est2Δ TEL1/tel1Δ* and *EST2/est2Δ TEL1/TEL1–hy184* diploids. Every 24 hr, cell concentrations and the corresponding PDs were determined, and samples were collected to determine cell viability before diluting cell cultures to the starting concentration of 5×10^4 cells/ml (Figure S1B). As expected, *est2Δ* cells showed a gradual reduction of cell density starting from ∼50 PDs (Figure 1A) until they reached the minimum cell density ("crisis" in Figure 1B) at ∼65 PDs, followed by restoration of nearly wild-type growth (Figure 1A). This latter growth phase was due to the accumulation of survivors that elongate their telomeres by telomerase-independent mechanisms and therefore reacquire replicative potential (Lundblad and Blackburn 1993). The absence of Tel1 delayed senescence of ∼10 PDs, with *est2Δ tel1Δ* cells reaching the minimum cell density at ∼74 PDs, as expected (Figure 1, A and B; Chang and Rothstein 2011). Conversely, *est2Δ TEL1–hy184* cells lost proliferative capacity ∼10 PDs earlier than *est2Δ* cells and reached the minimum cell density at ∼55 PDs (Figure 1, A and B). This early decrease in proliferative capacity was not due to a growth defect conferred by the *TEL1–hy184* mutation *per se*. In fact, *TEL1–hy184* cells showed constant growth rates after each dilution, similar to both wild-type and *tel1Δ* cells (Figure 1A). Furthermore, meiotic tetrads of *EST2/est2Δ TEL1/TEL1–hy184* diploids generated spore colonies of similar sizes independently of the presence of the *TEL1–hy184* allele (Figure 1C). Finally, *est2Δ TEL1–hy184* cells restored nearly wild-type growth after 90 PDs (Figure 1A), as expected in cases of accumulation of survivors.

A similar precocious decrease in proliferative capacity of *est2Δ TEL1–hy184* cells was also observed when the same cells were spotted out onto YEPD plates after each day of growth during the senescence assay. In fact, *est2Δ TEL1–hy184* strains showed a decrease in both colony size and density (Figure 1D), as well as a strong decrease in cell viability (Figure 1E and Figure S1C), starting from the first passage in liquid medium (∼40 PDs). In contrast, *est2Δ* cells generated smaller colonies than wild-type cells and showed loss of viability only after the second passage in liquid medium (∼50 PDs) (Figure 1, D and E and Figure S1C). The decreased cell growth in *est2Δ* and *est2Δ TEL1–hy184* cells correlated with an accumulation of cells with the same total amount of DNA (2C) as cells in G2 phase, as indicated by FACS analysis (Figure 1F). Furthermore, it was followed by the accumulation of survivors, as indicated by the appearance of colonies with wild-type size (Figure S1C), increased cell viability (Figure 1E and Figure S1C), and the bypass of the G2 block (Figure 1F). *TEL1–hy184* anticipated the onset of senescence of ∼10 PDs also in *tlc1Δ* cells, which lack the telomerase RNA moiety (Figure S2). Altogether, these results indicate that Tel1–hy184 accelerates senescence in the absence of telomerase, while the lack of Tel1 delays it.

The precocious senescence observed in *est2Δ TEL1–hy184* cells compared to *est2Δ* cells could be caused by accelerated telomere shortening and/or telomere loss. Therefore, we analyzed telomere length by Southern blot analysis with a TG-rich DNA probe as a function of PDs during the liquid senescence assay. Telomere shortening was not enhanced in *est2Δ TEL1–hy184* cells compared to *est2Δ* cells, and both strains showed telomeric signals until ∼60 PDs (Figure 1, G and H), although *est2Δ TEL1–hy184* cells had decreased cell proliferation at the same time points (Figure 1A). We can conclude that Tel1–hy184 induces a fast senescence, without accelerating the kinetics of bulk telomere shortening or telomere loss.

TEL1–hy184 does not increase ssDNA generation at telomeres

Tel1 is known to promote ssDNA generation at both DSBs and telomeres (Mantiero *et al.* 2007; Martina *et al.* 2012). As ssDNA triggers senescence (Abdallah *et al.* 2009; Khadaroo *et al.* 2009; Ballew and Lundblad 2013; Teixeira 2013; Fallet *et al.* 2014), the delayed senescence of telomerase-deficient *tel1Δ* cells might be due to a decrease in the amount of telomeric ssDNA (Gao *et al.* 2010; Ballew and Lundblad 2013; Fallet *et al.* 2014). If this were the case, Tel1–hy184 might

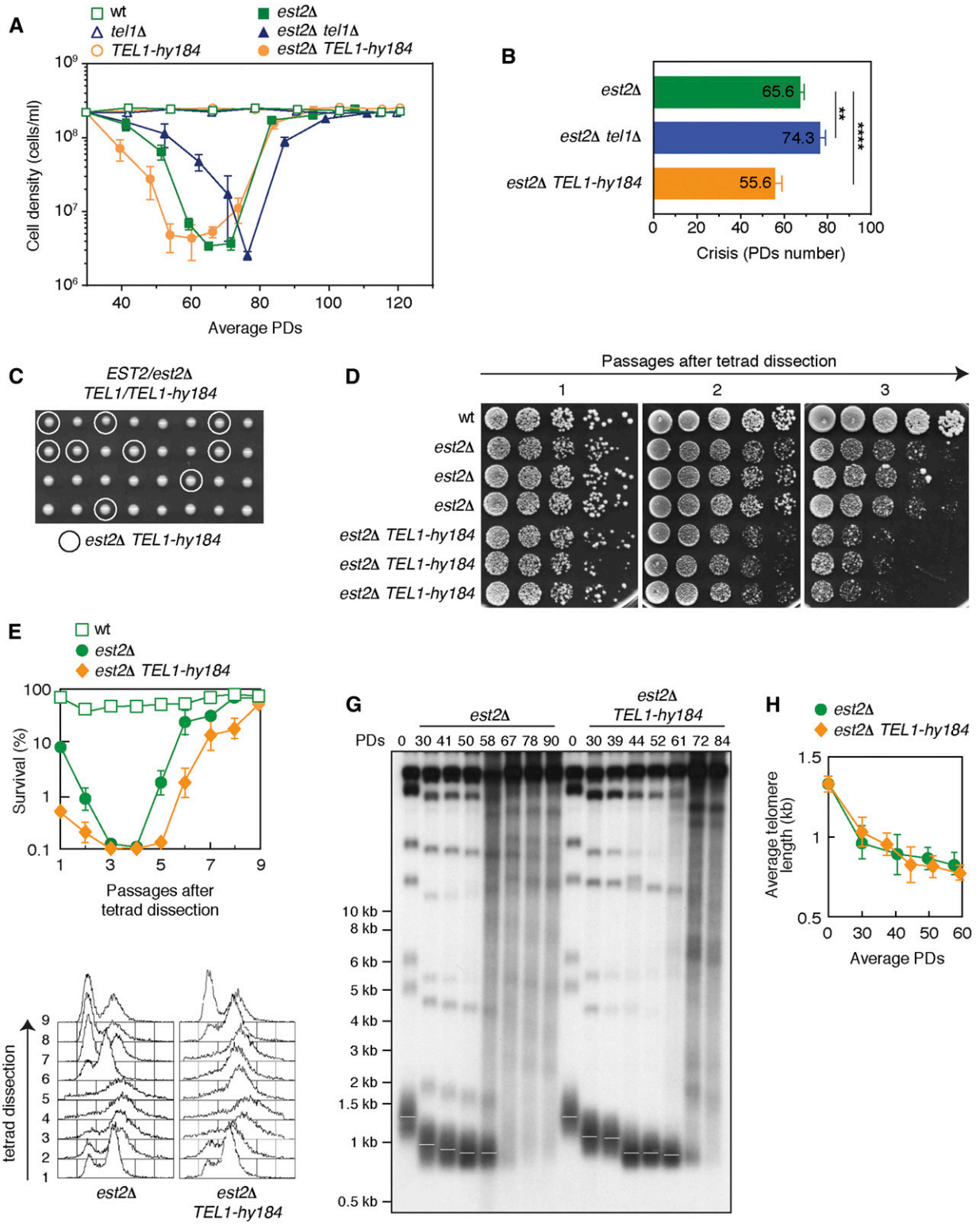

Figure 1 Effect of *tel1*Δ and *TEL–hy184* on replicative senescence. (A–H) After tetrad dissection, spore clones were grown for 48 hr at 30° onto YEPD plates and then transferred to liquid culture. Every 24 hr, cell cultures were diluted back to 5×10^4 cells/ml in YEPD. (A) The mean cell concentrations of independent clones with the same genotypes after each day of growth against the number of PDs since tetrad dissection were plotted. We assumed that the spores had undergone 30 PDs before the first density measurement. Error bars denote SD. (B) The mean PD numbers at the peak of senescence (crisis) for each genotype are represented. Error bars denote SD. Wild-type, $n = 3$; *tel1*Δ, $n = 3$; *TEL1–hy184*, $n = 3$; *est2*Δ, $n = 5$; *est2*Δ *tel1*Δ, $n = 4$; and *est2*Δ *TEL1–hy184*, $n = 7$. Student's *t*–test: ** $P < 0.01$ and **** $P < 0.0001$. (C) Meiotic tetrads from the indicated diploids were dissected on YEPD plates that were incubated at 30° for 48 hr, followed by spore genotyping. (D and E) Cell samples harvested daily since the first passage in liquid medium (~30 PDs after tetrad dissection) were serially diluted (1:10) before being spotted out onto YEPD plates (D), or plated onto YEPD plates to determine the

anticipate senescence by increasing ssDNA accumulation at telomeres. Exo1 exonuclease is known to promote the generation of ssDNA at unprotected telomeres (Fallet *et al.* 2014) and the lack of Exo1 slightly delays senescence (Dewar and Lydall 2010; Fallet *et al.* 2014; Hardy *et al.* 2014). The helicase Sgs1 also contributes to induce senescence (Hardy *et al.* 2014) and promotes DNA-end processing by acting in a different pathway to that of Exo1 (Villa *et al.* 2016). We asked whether the accelerated senescence of *est2*Δ *TEL1–hy184* cells depends on Exo1 and/or Sgs1. We used the separation-of-function *sgs1–D664*Δ allele, which delays senescence in *est2*Δ cells and causes defects in DNA-end processing, but not in the resolution of recombination intermediates (Bernstein *et al.* 2009; Hardy *et al.* 2014). *EXO1* deletion delayed senescence onset in *est2*Δ cells of ∼10 PDs, while it did not significantly delay senescence in *est2*Δ *TEL1–hy184* cells (Figure 2A). In fact, while the decline in cell proliferation appeared to be slightly slower in *est2*Δ *TEL1–hy184 exo1*Δ cells than in *est2*Δ *TEL1–hy184* cells (Figure 2A), the two strains reached the minimum cell density after similar mean numbers of PDs (Figure 2B). Furthermore, the proliferative decline of *est2*Δ *TEL1–hy184* cells was not delayed by the *sgs1–D664*Δ allele, both in the presence and in the absence of Exo1 (Figure 2C). Therefore, Exo1 and Sgs1 do not account for the anticipated senescence induced by Tel1–hy184.

Telomeric ssDNA generation depends also on the MRX complex, whose activity at telomeres is regulated in an opposing manner by Tel1 and Rif2. Rif2 prevents telomere processing by limiting MRX accumulation at chromosome ends (Bonetti *et al.* 2010). In contrast, Tel1, once recruited to DNA ends by MRX, enhances ssDNA generation at telomeres by promoting MRX association to DNA ends in a positive feedback loop (Martina *et al.* 2012). Both Tel1 and Rif2 interact with the C-terminus of the MRX subunit Xrs2, suggesting that Rif2 and Tel1 compete with each other for MRX binding (Nakada *et al.* 2003; Hirano *et al.* 2009; Martina *et al.* 2012). Therefore, we asked whether Tel1–hy184 induces fast senescence by overcoming the inhibition that Rif2 exerts on MRX. *est2*Δ *TEL1–hy184 rif2*Δ cells decreased cell proliferation faster than either *est2*Δ *TEL1–hy184* or *est2*Δ *rif2*Δ cells, which both anticipated the onset of senescence of ∼10 PDs compared to *est2*Δ cells (Figure 2, D and E). These results suggest that the lack of Rif2 and the presence of Tel1–hy184 promote senescence by affecting different pathways, and that Tel1 might play an additional function in modulating the onset of senescence that is different from the induction of MRX-dependent ssDNA.

We then directly monitored ssDNA at native telomeres after telomerase inactivation. Genomic DNA prepared from telomerase-negative spore clones was analyzed by nondenaturing in-gel hybridization with a CA-rich radiolabeled oligonucleotide that detects TG-rich ssDNA (Dionne and Wellinger 1996). The total amount of TG repeats was detected by the same probe after denaturation of the gel. As expected, the levels of TG-rich ssDNA signals were higher in *est2*Δ cells compared to wild-type *EST2* cells 3 days after tetrad dissection, due to telomere erosion after telomerase inactivation (Figure S3, A and B). Both the ssDNA signals (native) and the TG repeats signals (denatured) decreased during the experiment, as expected from the progressive loss of telomeric sequences in the absence of telomerase (Figure 3, A and B). *est2*Δ *TEL1–hy184* cells did not show increased levels of TG-rich ssDNA signals compared to *est2*Δ *TEL1* cells (Figure 3, A and B), supporting the hypothesis that the anticipated senescence triggered by the Tel1–hy184 variant is not caused by increased telomere processing.

As ssDNA is generated very fast at the TG-rich telomeric sequences after telomerase inactivation, we quantified ssDNA during senescence at internal X subtelomeric DNA sequences by QAOS (Booth *et al.* 2001; Zubko *et al.* 2006). As a control, we monitored ssDNA at X sequences in *est2*Δ *rif2*Δ cells, which are expected to enhance ssDNA (Abdallah *et al.* 2009; Khadaroo *et al.* 2009; Bonetti *et al.* 2010; Ballew and Lundblad 2013). Processing of X sequences was not enhanced by Tel1–hy184. Both *est2*Δ and *est2*Δ *TEL1–hy184* cells showed almost 5–7% of ssDNA at subtelomeric sequences after tetrad dissection, while almost 10–15% of ssDNA was detectable in the same regions in *est2*Δ *rif2*Δ cells derived from the same diploid (Figure 3C). Furthermore, Tel1–hy184 did not reduce the viability of cells carrying the *cdc13–1* temperature-sensitive allele (Figure S3C), which causes cell lethality at high temperatures because of the accumulation of ssDNA at chromosomal DNA ends (Garvik *et al.* 1995; Vodenicharov and Wellinger 2006). This finding suggests that Tel1–hy184 does not enhance DNA degradation when chromosome-end capping is defective.

We confirmed that Tel1–hy184 has no effect on telomeric ssDNA by evaluating ssDNA generation at an HO-inducible short telomere, whose processing is known to be promoted by Tel1 (Martina *et al.* 2012). We inserted the *TEL1–hy184* allele in a yeast strain carrying an 81-bp TG repeats sequence placed immediately adjacent to an HO endonuclease recognition sequence at the *ADH4* locus on chromosome VII. This strain expresses the *HO* gene from a galactose-inducible *GAL1* promoter (Diede and Gottschling 1999). HO cleavage creates a centromere-proximal TG-rich DNA end, whose processing can be evaluated by Southern blot under denaturing conditions using a single-stranded RNA probe that anneals to the 5′ CA-rich strand. The HO cleavage converts the uncut

colony-forming units (E). Plotted values are the mean values of independent clones with the same genotypes as in (B). Error bars denote SD. (F–H) Cell samples harvested daily since the first passage in liquid medium were subjected to FACS analysis of DNA content (F) or Southern blot analysis with a poly(GT) probe (G). The mean lengths of telomeres at different time points were determined from Southern blots (H). Error bars denote SD (n = 3). PDs, population doublings; wt, wild-type; YEPD, Yep medium supplemented with 2% glucose.

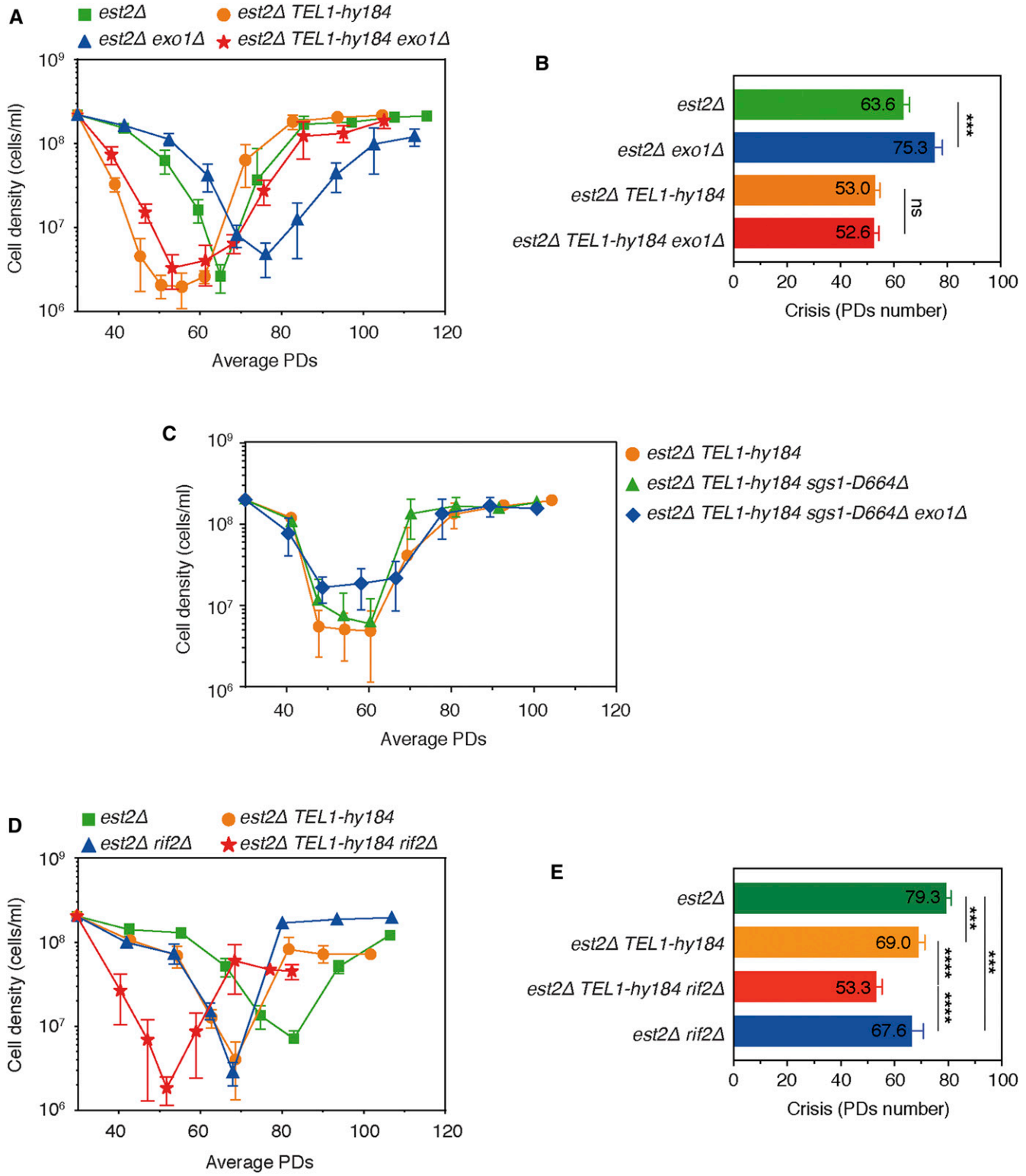

Figure 2 *Exo*1 and *Sgs*1 are not responsible for precocious senescence induced by Tel1–hy184. (A–E) Senescence assays were performed as in Figure 1A. (A, C, and D) The mean cell concentrations of independent clones with the same genotypes against PDs were plotted. Error bars denote SD. (B and E) The mean PD numbers at the peak of senescence (crisis) for each genotype are represented. Error bars denote SD. Student's *t*-test: *** $P < 0.001$ and **** $P < 0.0001$. (A and B) *est2*Δ, $n = 4$; *est2*Δ *TEL1–hy184*, $n = 4$; *est2*Δ *exo1*Δ, $n = 4$; and *est2*Δ *TEL1–hy184 exo1*Δ, $n = 5$. (C) *est2*Δ *TEL1–hy184*, $n = 4$; *est2*Δ *TEL1–hy184 sgs1–D664*Δ, $n = 4$; and *est2*Δ *TEL1–hy184 sgs1–D664*Δ *exo1*Δ, $n = 4$. (D and E) *est2*Δ, $n = 4$; *est2*Δ *TEL1–hy184*, $n = 6$; *est2*Δ *rif2*Δ, $n = 6$; and *est2*Δ *TEL1–hy184 rif2*Δ, $n = 9$. ns, not significant; PDs, population doublings.

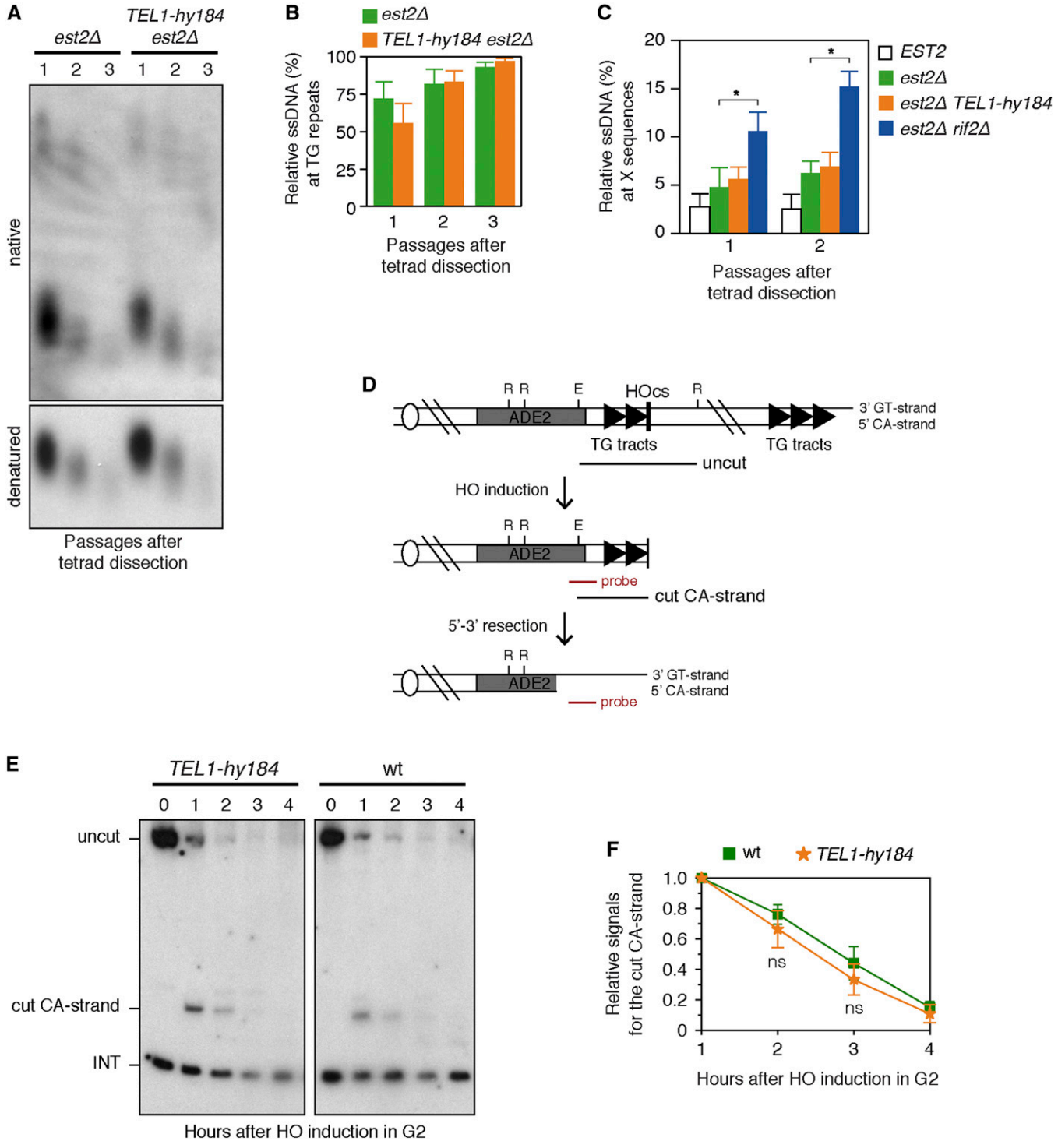

Figure 3 Tel1–hy184 does not affect the generation of ssDNA at telomeres. (A–C) Senescence assays were performed as in Figure 1A. (A) Genomic DNA extracted from cell samples harvested daily since the first passage in liquid medium (~30 PDs) was digested with *Xho*I and subjected to nondenaturing in-gel hybridization using an end-labeled CA-rich oligonucleotide as a probe (native). The gel was then denatured and hybridized with the same CA-rich probe (denatured). (B) Densitometric analysis. The amount of native TG-ssDNA was normalized to the total amount of TG sequences for each sample. Plotted values are the mean value ± SD from three independent experiments as in (A). (C) ssDNA quantity was monitored by QAOS using primers located in the subtelomeric X repeats. Plotted values are the mean value ± SD (n = 3). Student's t-test: * $P < 0.05$. (D) Schematic representation of the HO-inducible telomere system. Galactose-induced HO endonuclease generates a DSB at a HOcs adjacent to an 81-bp TG repeats sequence (TG tracts) that is inserted at the *ADH4* locus on chromosome VII. *Rsa*I (R)- and *Eco*RV (E)-digested genomic DNA was hybridized with a single-stranded riboprobe (in red), which anneals to the 5′ CA-strand 212 bp from HOcs. The probe reveals an uncut 390-nt DNA fragment (uncut), which is converted by HO cleavage into a 166-nt fragment (cut CA-strand). Degradation of the 5′ CA-strand leads to disappearance of this signal. The probe also

390-nt DNA fragment revealed by this probe into a 166-nt fragment (cut CA-strand), whose subsequent disappearance indicates that the 5′ strand degradation has proceeded beyond the hybridization region (Figure 3D). To avoid possible effects on ssDNA generation due to different cell cycle phases, we evaluated processing of the TG-rich end generated after the HO cleavage in wild-type and *TEL1–hy184* cells kept arrested in G2 with nocodazole. The band corresponding to the cut CA-rich strand disappeared with similar kinetics in both wild-type and *TEL1–hy184* cells (Figure 3, E and F), indicating that Tel1–hy184 does not affect the processing of an HO-induced short telomere. Altogether, these results indicate that the Tel1–hy184 variant does not accelerate senescence by increasing ssDNA generation at telomeres.

Tel1 kinase activity is required to induce senescence, while it is dispensable for telomere processing

Tel1 plays both kinase-dependent and -independent functions. Tel1 kinase activity is required for both telomere elongation and checkpoint activation (Greenwell *et al.* 1995; Mallory and Petes 2000; Gobbini *et al.* 2015), while it is dispensable for the association of Tel1 and MRX to telomeres, and for Tel1-mediated processing of DSB ends (Takata *et al.* 2004; Hirano *et al.* 2009; Gobbini *et al.* 2015; Cassani *et al.* 2016). To assess whether Te1l kinase activity is necessary to support the role of Tel1 in promoting senescence, we analyzed replicative senescence in the presence of the *tel1–kd* allele, which carries the G2611D, D2612A, N2616K, and D2631E amino acid substitutions that abolish Tel1 kinase activity *in vitro* (Mallory and Petes 2000). As Tel1 promotes the nucleolytic degradation of DSB ends independently of its kinase activity (Gobbini *et al.* 2015; Cassani *et al.* 2016), we first analyzed nucleolytic degradation of the HO-induced telomere in the presence of the *tel1–kd* allele. The cut CA-strand signals disappeared with similar kinetics in both wild-type and *tel1–kd* cells, while they persisted longer in *tel1*Δ cells, as expected (Figure 4, A and B; Martina *et al.* 2012). Similar results were obtained at native telomeres, as the amount of TG-rich ssDNA was similar in senescing *est2*Δ and *est2*Δ *tel1–kd* cells, while it was slightly reduced in *est2*Δ *tel1*Δ cells compared to *est2*Δ cells (Figure 4, C and D). *tel1*Δ cells also accumulated less ssDNA compared to *est2*Δ and *est2*Δ *tel1–kd* cells at subtelomeric X sequences, where similar levels of ssDNA were measured in both *est2*Δ and *est2*Δ *tel1–kd* cells (Figure 4E). Therefore, Tel1 stimulates the degradation of telomeric DNA independently of its kinase activity.

Importantly, *est2*Δ *tel1–kd* cells decreased their proliferation capacity starting from 55 PDs and reached the minimum cell density at 73 PDs, ∼10 PDs later than *est2*Δ cells (Figure 4, F and G). As the lack of Tel1 kinase activity did not affect the generation of ssDNA at telomeres in *est2*Δ cells (Figure 4, C–E), these results indicate that Tel1 kinase activity promotes replicative senescence in the presence of wild-type levels of telomeric ssDNA. However, senescence appeared to be anticipated of ∼5 PDs in *est2*Δ *tel1–kd* cells compared to *est2*Δ *tel1*Δ cells (Figure 4, F and G). Therefore, while Tel1 kinase activity strongly contributes to senescence induction, kinase-independent functions of Tel1 are likely involved in the same process. Altogether, these data indicate that the main function of Tel1 in promoting replicative senescence requires Tel1 kinase activity and that it is not related to the generation of ssDNA at telomeres.

Precocious senescence in TEL1–hy184 cells is triggered by the activation of a DNA damage checkpoint that depends totally on Rad9 and only partially on Mec1

The decrease in cell density after telomerase inactivation correlates with checkpoint activation that depends on both Rad9 and Mec1 (Enomoto *et al.* 2002; IJpma and Greider 2003). We asked whether the fast senescence promoted by the *TEL1–hy184* allele depends on checkpoint activation by performing a senescence assay in telomerase-negative cells and monitoring Rad53 phosphorylation, which is a marker of checkpoint activation and is induced in senescing telomerase-negative cells (IJpma and Greider 2003). Mobility shifts corresponding to Rad53 phosphorylated forms were detectable by western blot in both *est2*Δ and *est2*Δ *TEL1–hy184* cell extracts after two-to-three passages of spore clones in liquid culture, while they were under the detection level in *est2*Δ *rad9*Δ and *est2*Δ *TEL1–hy184 rad9*Δ cells (Figure 5A), indicating that a Rad9- and Rad53-dependent checkpoint is activated in senescing *est2*Δ and *est2*Δ *TEL1–hy184* cells. This checkpoint activation accounts for the senescence kinetics of *est2*Δ and *est2*Δ *TEL1–hy184* cells. In fact, both *est2*Δ *rad9*Δ and *est2*Δ *TEL1–hy184 rad9*Δ cells reduced cell density starting from ∼60 PDs, and reached the minimum cell density at ∼75 PDs, ∼10 PDs later than *est2*Δ cells and 20 PDs later than *est2*Δ *TEL1–hy184* cells (Figure 5B).

The lack of Rad9 also completely relieved the precocious senescence caused by the *TEL1–hy184* allele in cells lacking *TLC1* (Figure S4A), and abolished Rad53 phosphorylation in both *tlc1*Δ and *tlc1*Δ *TEL1–hy184* cells (Figure S4B). Furthermore, Rad9 contributes to reduce the growth of *est2*Δ *TEL1–hy184* cells spotted out onto YEPD plates, as *est2*Δ *TEL1–hy184* cells showed small colonies starting from the first passage after sporulation, while a decrease in colony number and size was detectable in *est2*Δ *TEL1–hy184 rad9*Δ

detects a 138-nt fragment from the *ade2–101* locus on chromosome XV, which serves as an INT. (E) HO expression was induced at time zero by galactose addition to nocodazole-arrested cell cultures that were kept arrested in G2. Genomic DNA was subjected to Southern blot analysis as described in (D). (F) Densitometric analysis. The cut CA-strand signals were normalized to the INT signals for each time point. Plotted values are the mean value ± SD from three independent experiments as in (E). DSB, double-strand break; HO, HOmothallic switching endonuclease; HOcs, HO cleavage site; INT, internal loading control; ns, not significant; PDs, population doublings; QAOS, quantitative amplification of ssDNA; ssDNA, single-stranded DNA; wt, wild-type.

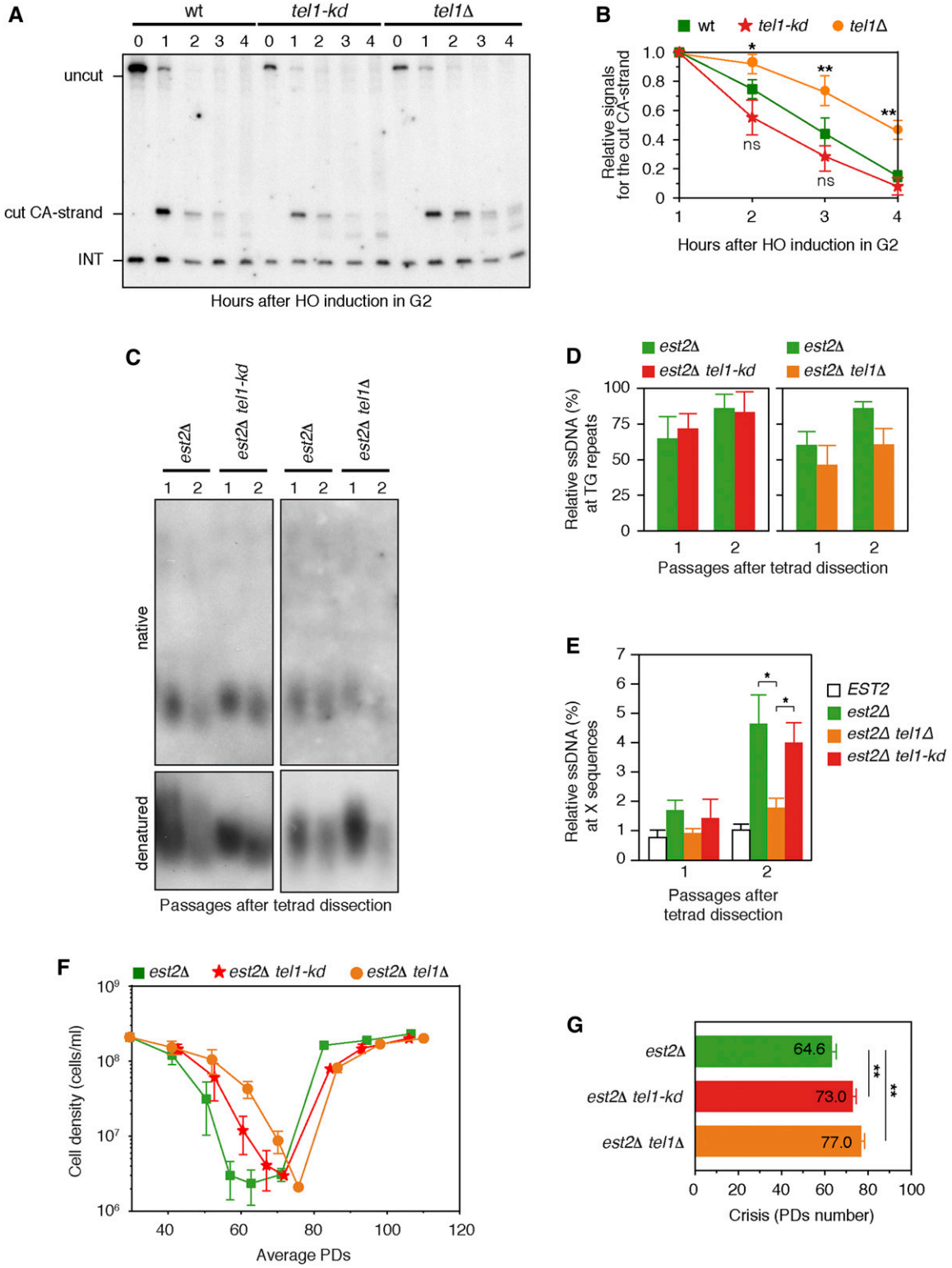

Figure 4 Tel1–kd delays senescence without affecting telomeric ssDNA generation. (A) HO expression was induced at time zero by galactose addition to nocodazole-arrested cell cultures that were kept arrested in G2. Genomic DNA was analyzed by Southern blot under denaturing conditions as in Figure 3D. (B) Densitometric analysis. Plotted values are the mean value ± SD from three independent experiments as in (A). (C) *Xho*I-digested genomic DNA extracted from cell samples harvested daily since the first passage in liquid medium (~30 PDs) was subjected to nondenaturing in-gel hybridization as in Figure 3A. (D) Densitometric analysis. Plotted values are the mean value ± SD from three independent experiments as in (C). (E) ssDNA quantity was monitored by QAOS using primers located in the subtelomeric X repeats. Plotted values are the mean value ± SD (n = 3). (F and G) Senescence assay as in Figure 1A. (F) The mean cell concentration of independent clones with the same genotype against PDs was plotted. (G) The mean PD

cells only starting from the second passage in liquid medium (Figure 5C). Thus, the precocious senescence induced by the Tel1–hy184 variant appears to depend on the activation of a Rad9-dependent checkpoint. Although many more replicates would be required to make these observations statistically significant, Rad53 phosphorylation appeared earlier and persisted longer in *est2*Δ *TEL1–hy184* cells than in *est2*Δ cells (Figure 5A). Furthermore, the arrest of cell proliferation, which was anticipated in *est2*Δ *TEL1–hy184* cells compared to *est2*Δ cells, persisted on average slightly longer in *est2*Δ *TEL1–hy184* than in *est2*Δ cells (Figure 1, A and F, Figure 2A, and Figure 5B). Finally, the *TEL1–hy184* allele appeared to promote Rad53 phosphorylation, cell cycle arrest, and the decrease of cell proliferation in the *est2*Δ background when telomeres did not look so deranged as in *est2*Δ *TEL1* cells (Figure 1 and Figure 5A). Altogether, these observations suggest that the Tel1–hy184 variant may decrease the threshold of telomeric signals required for checkpoint activation in the absence of telomerase.

As Tel1–hy184 decreases cell viability in the absence of telomerase in a Rad9-dependent manner (Figure 5C), we asked whether Tel1–hy184 also affects cell viability in response to DNA damage both in the presence and absence of Rad9. While the lack of Tel1 causes sensitivity to the topoisomerase inhibitor camptothecin (CPT) (Figure 5D; Menin *et al.* 2018), *TEL1–hy184* cells were resistant to CPT and MMS, and showed only mild sensitivity to the radiomimetic drug phleomycin (Phleo) (Figure 5D), suggesting that Tel1–hy184 might impair the response to DNA DSBs. However, we were unable to define whether this sensitivity depends on Rad9 because the lack of Rad9 *per se* caused phleomycin sensitivity (Figure 5E).

Tel1 contributes to checkpoint activation both by generating ssDNA that activates Mec1 and by acting in a pathway parallel to Mec1 (Clerici *et al.* 2004; Mantiero *et al.* 2007). We tested whether Mec1 is required for the anticipated senescence induced by Tel1–hy184 by repeating the senescence assay in telomerase-negative cells lacking Mec1 (kept viable by the lack of the ribonucleotide reductase inhibitor Sml1). As expected, senescence onset was delayed by ∼10 PDs in *est2*Δ *mec1*Δ cells compared to *est2*Δ cells (Figure 5F). Interestingly, *est2*Δ *TEL1–hy184 mec1*Δ cells lost proliferative capacity ∼10 PDs earlier than *est2*Δ *mec1*Δ cells (Figure 5F), indicating that Tel1–hy184 also anticipates senescence in the absence of Mec1. The same effect was observed in a *tlc1*Δ background. In fact, *tlc1*Δ *TEL1–hy184 mec1*Δ cells decreased cell proliferation ∼10 PDs earlier than *tlc1*Δ *mec1*Δ cells (Figure S4C). Furthermore, Rad53 phosphorylation, which was under the detection level in both *est2*Δ *mec1*Δ (Figure 5G) and *tlc1*Δ *mec1*Δ cells (Figure S4D), was still detectable in senescing *est2*Δ *TEL1–hy184 mec1*Δ (Figure 5G) and *tlc1*Δ *TEL1–hy184 mec1*Δ cells (Figure S4D), although to a lesser extent than in *est2*Δ *TEL1–hy184* and *tlc1*Δ *TEL1–hy184* cells (Figure 5G and Figure S4D). These results indicate that Tel1–hy184 can promote Rad53 phosphorylation independently of Mec1. Consistent with a decreased Rad53 phosphorylation in both *est2*Δ *TEL1–hy184 mec1*Δ and *tlc1*Δ *TEL1–hy184 mec1*Δ cells, compared to *est2*Δ *TEL1–hy184* cells and *tlc1*Δ *TEL1–hy184* cells (Figure 5G and Figure S4D), senescence was slower in *est2*Δ *TEL1–hy184 mec1*Δ and *tlc1*Δ *TEL1–hy184 mec1*Δ cells than in *est2*Δ *TEL1–hy184* and *tlc1*Δ *TEL1–hy184* cells, respectively (Figure 5F and Figure S4C). Thus, Mec1 partially contributes to the reduction of cell proliferation in telomerase-deficient cells expressing the Tel1–hy184 variant, which appears to activate a Rad9-dependent checkpoint in both a Mec1-dependent and -independent manner.

*The amino acid substitutions located in the FRAP–ATM–TRAPP domain are responsible for early senescence of TEL1–hy184 est2*Δ *cells*

The Tel1–hy184 variant carries five amino acid substitutions grouped in two different clusters. Two substitutions (R2735G and E2737V) are located in the C-terminal kinase domain, while the other three substitutions (F1752I, D1985N, and E2133K) are grouped in the conserved FRAP–ATM–TRAPP (FAT) domain (Figure 6A). To understand which group of substitutions was responsible for the precocious senescence triggered by Tel1–hy184, we constructed the *TEL1–hy184–3N* allele, which carried the F1752I, D1985N, and E2133K amino acid substitutions, and the *TEL1–hy184–2C* allele, which carried the R2735G and E2737V substitutions (Figure 6A). Interestingly, both *TEL1–hy184–3N* and *TEL1–hy184–2C* alleles suppressed the hypersensitivity of *mec1*Δ cells to HU similar to *TEL1–hy184* (Figure 6B), indicating that each group of mutations is sufficient to compensate for the lack of Mec1 functions in HU.

Tel1–hy184 was shown to possess an intrinsic kinase activity similar or maybe slightly higher than wild-type Tel1, and to cause mild telomere overelongation (Baldo *et al.* 2008). After immunoprecipitation with anti-HA antibodies of different Tel1 variants from cells expressing fully functional *TEL1*, *TEL1–HA*, *TEL1–hy184–HA*, *TEL1–hy184–3N–HA*, or *TEL1–hy184–2C–HA* alleles, we measured their *in vitro* kinase activity on the artificial substrate of the ATM kinase family, PHAS-I (Mallory and Petes 2000; Baldo *et al.* 2008). The Tel1–hy184 variant turned out to have a higher intrinsic kinase activity than wild-type Tel1 and the mutations in the kinase domain were responsible for it. In fact, the amount of phosphorylated PHAS-I in the presence of Tel1–hy184–HA or Tel1–hy184–2C–HA was 12–16-fold higher than in the presence of Tel1–HA (Figure 6C), while a similar amount of phosphorylated PHAS-I was detectable in

numbers at the peak of senescence (crisis) for each genotype are represented. Error bars denote SD. *est2*Δ, $n = 6$; *est2*Δ *tel1*Δ, $n = 6$; and *est2*Δ *Tel1–kd*, $n = 6$. Student's *t*-test: * $P < 0.05$ and ** $P < 0.01$. HO, HOmothallic switching endonuclease; INT, internal loading control; ns, not significant; PDs, population doublings; QAOS, quantitative amplification of ssDNA; ssDNA, single-stranded DNA; wt, wild-type.

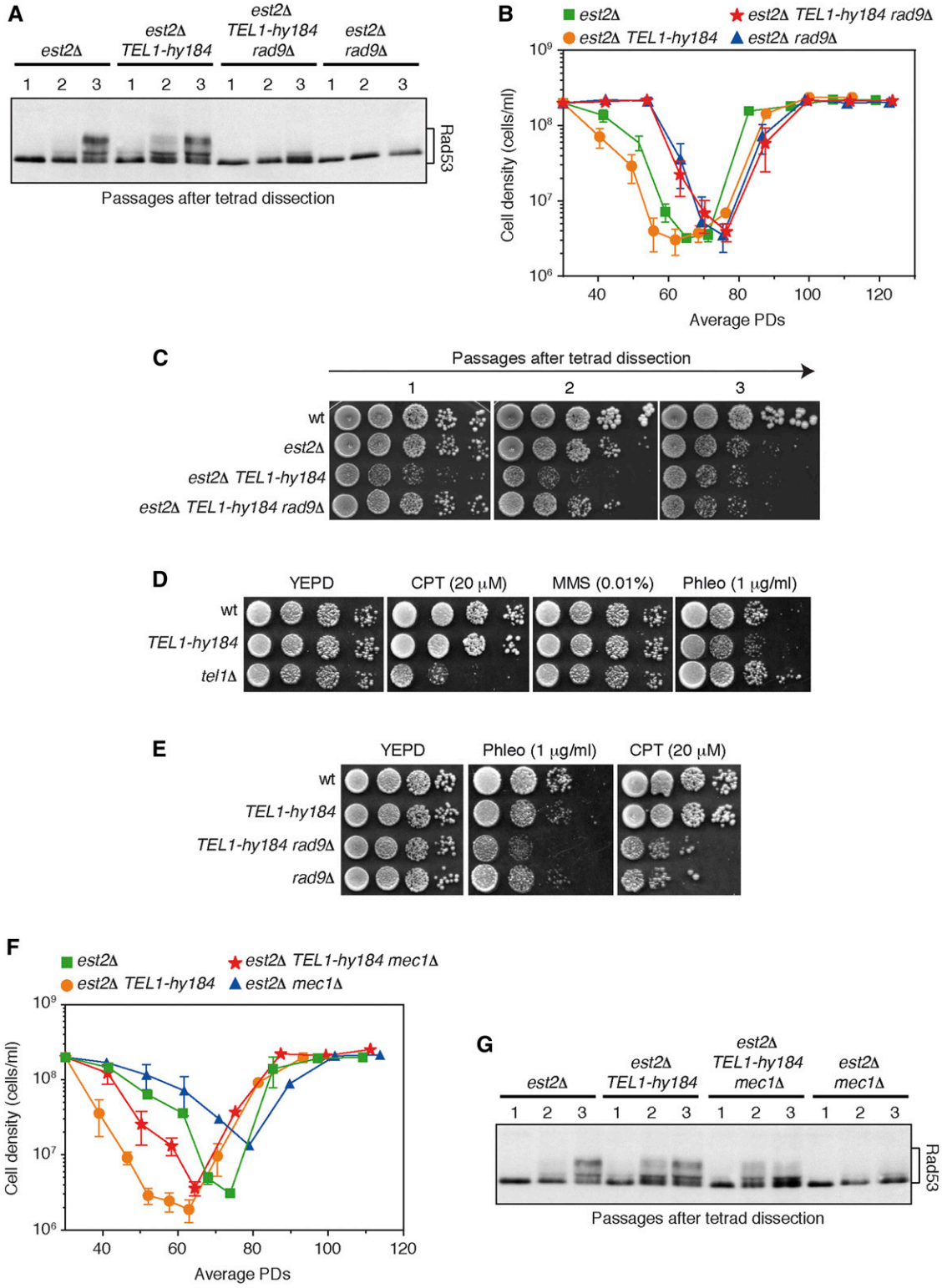

Figure 5 The precocious senescence induced by Tel1–hy184 requires Rad9 and only partially Mec1. (A–C) Senescence assays were performed as in Figure 1A. (A) Protein extracts prepared from cell samples harvested daily since the first passage in liquid medium (~30 PDs) were analyzed by western blot with anti-Rad53 antibodies. (B) The mean cell concentrations of independent clones with the same genotypes against PDs were plotted. Error bars denote SD. *est2*Δ, $n = 4$; *est2*Δ *TEL1–hy184*, $n = 4$ *est2*Δ *rad9*Δ, $n = 6$; and *est2*Δ *TEL1–hy184 rad9*Δ, $n = 6$. (C) Cell samples harvested daily since the first passage in liquid medium were serially diluted (1:10) before being spotted out onto YEPD plates. (D and E) Exponentially growing cell cultures were serially diluted (1:10) and each dilution was spotted out onto YEPD plates, with or without (CPT), MMS, and Phleo. (F and G) Senescence assays were

the presence of Tel1–hy184–3N–HA or Tel1–HA (Figure 6C). PHAS-I phosphorylation depends on Tel1, as it was not detected in the presence of untagged Tel1 (Figure 6C).

Consistent with previous conclusions that telomere elongation depends on Tel1 kinase activity (Greenwell *et al.* 1995; Mallory and Petes 2000; Baldo *et al.* 2008; Martina *et al.* 2012), both *TEL1–hy184* and *TEL1–hy184–2C* alleles, which increased Tel1 kinase activity (Figure 6C), caused a mild telomere overelongation in the *mec1*Δ background compared to both wild-type and *mec1*Δ cells (Figure 6D). Conversely, telomeres were of wild-type length in the presence of the *TEL1–hy184–3N* allele (Figure 6D), which did not increase Tel1 kinase activity (Figure 6C).

We then assayed the senescence kinetics of *est2*Δ *TEL1–hy184–3N* and *est2*Δ *TEL1–hy184–2C* cells, compared to *est2*Δ cells, after sporulation and tetrad dissection of *EST2/est2*Δ *TEL1/TEL1–hy184–3N* or *EST2/est2*Δ *TEL1/TEL1–hy184–2C* diploids, respectively. *est2*Δ *TEL1–hy184–2C* cells appeared to slightly anticipate the decrease in cell proliferation compared to *est2*Δ cells, although the difference in the mean number of PDs carried out by the two strains before reaching the minimum cell density was not statistically significant (Figure 6, E and G). Conversely, *est2*Δ *TEL1–hy184–3N* cells decreased proliferative capacity starting from ∼47 PDs and reached the minimum cell density at ∼57 PDs, almost 10 PDs earlier than *est2*Δ cells derived from the same diploid (Figure 6, F and H), indicating that precocious senescence is mainly caused by the F1752I, D1985N, and E2133K substitutions.

Tel1–hy184–3N binds telomeric DNA ends more robustly than wild-type Tel1

The finding that Tel1–hy184 can promote the activation of a Rad9-dependent checkpoint in telomerase-negative cells independently of Mec1 suggests that Tel1 may generate a checkpoint signal by itself at telomeres, and that the Tel1 variants with mutations in the FAT domain accelerate replicative senescence by doing it more efficiently. One possibility is that Tel1–hy184–3N is more robustly associated with short telomeres compared to wild-type Tel1, prompting us to evaluate the recruitment of Tel1 and Tel1–hy184–3N to an HO-induced telomere. The Tel1–HA and Tel1–hy184–3N–HA variants were expressed in the strain carrying both the 81-bp TG repeats adjacent to the HO-cutting site, at the *ADH4* locus and the *GAL1–HO* inducible gene (Diede and Gottschling 1999). Upon HO induction in G2-arrested cells, we performed ChIP followed by quantitative PCR with primer pairs located at both the telomeric (TG–HO) and HO sides of the HO-cutting site (Figure 7A). As expected, wild-type Tel1–HA associated with both sides of the HO-induced DSB, with a reduced amount of Tel1–HA bound to the TG–HO side compared to the amount associated with the nontelomeric HO side (Figure 7B; Hirano *et al.* 2009; Martina *et al.* 2012). The levels of the Tel1–hy184–3N–HA variant bound at both sides of the HO-induced DSB were higher compared to that of Tel1–HA (Figure 7B). This increased association cannot be ascribed to increased protein level, as similar amounts of Tel1–HA and Tel1–hy184–3N–HA could be detected in total protein extracts (Figure 7C).

We attempted to evaluate whether the F1752I, D1985N, and E2133K amino acid substitutions can also increase Tel1 binding at native telomeres. We were unable to detect Tel1–HA and Tel1–hy184–3N–HA enrichment at native telomeres by ChIP analysis even during a synchronous cell cycle, likely because only few Tel1 molecules bind native telomeres during a normal S phase. As an increased Tel1 binding to DNA ends results in an enhanced recruitment of MRX to the same ends (Hirano *et al.* 2009; Martina *et al.* 2012), we evaluated the amount of the MRX subunit Mre11 bound at native telomeres in *TEL1* and *TEL1–hy184–3N* cells synchronously released into the cell cycle from a G1 arrest. Similar amounts of Mre11–Myc were detected in protein extracts from *TEL1* and *TEL1–hy184–3N* cells (Figure 7D). Mre11 binding to VI–R telomere peaked in both *TEL1* and *TEL1–hy184–3N* cells 45 min after release, when the DNA was almost fully duplicated (Figure 7, E and F). However, the amount of Mre11 bound to this telomere was higher in *TEL1–hy184–3N* cells than in *TEL1* cells, indicating that Tel1–hy184–3N can enhance the association to native telomeres of MRX and likely of Tel1–hy184–3N itself. These findings, together with the observation that Tel1–hy184–3N increases neither Tel1 kinase activity (Figure 6C) nor telomere length (Figure 6D), suggest that Tel1–hy184 promotes replicative senescence by increasing Tel1 binding/persistence at DNA ends.

Discussion

The lack of Tel1 delays senescence (Ritchie *et al.* 1999; Enomoto *et al.* 2002; Abdallah *et al.* 2009; Gao *et al.* 2010; Chang and Rothstein 2011; Ballew and Lundblad 2013), and causes both a defect in checkpoint signaling (D'Amours and Jackson 2001; Clerici *et al.* 2004; Mantiero *et al.* 2007; Gobbini *et al.* 2015) and a delay in the processing of DNA ends (Mantiero *et al.* 2007; Martina *et al.* 2012). This double role of Tel1 in checkpoint signaling and DNA-end processing makes it difficult to define whether Tel1's function in promoting senescence can be ascribed either to a direct role of Tel1 in signaling critically short telomeres to the checkpoint, or rather to the generation of telomeric ssDNA that induces cell cycle arrest through the activation of a Mec1-dependent checkpoint.

Here, we analyzed the function of Tel1 in inducing senescence by taking advantage of two different *TEL1* alleles: the

performed as in Figure 1A. (F) The mean cell concentrations of independent clones with the same genotypes against PDs were plotted. Error bars denote SD. *est2*Δ, $n = 4$; *est2*Δ *TEL1–hy184*, $n = 4$ *est2*Δ *mec1*Δ, $n = 6$; and *est2*Δ *TEL1–hy184 mec1*Δ, $n = 8$. (G) Western blot with anti-Rad53 antibodies as in (A). CPT, camptothecin; PDs, population doublings; Phleo, phleomycin; wt, wild-type; YEPD, Yep medium supplemented with 2% glucose.

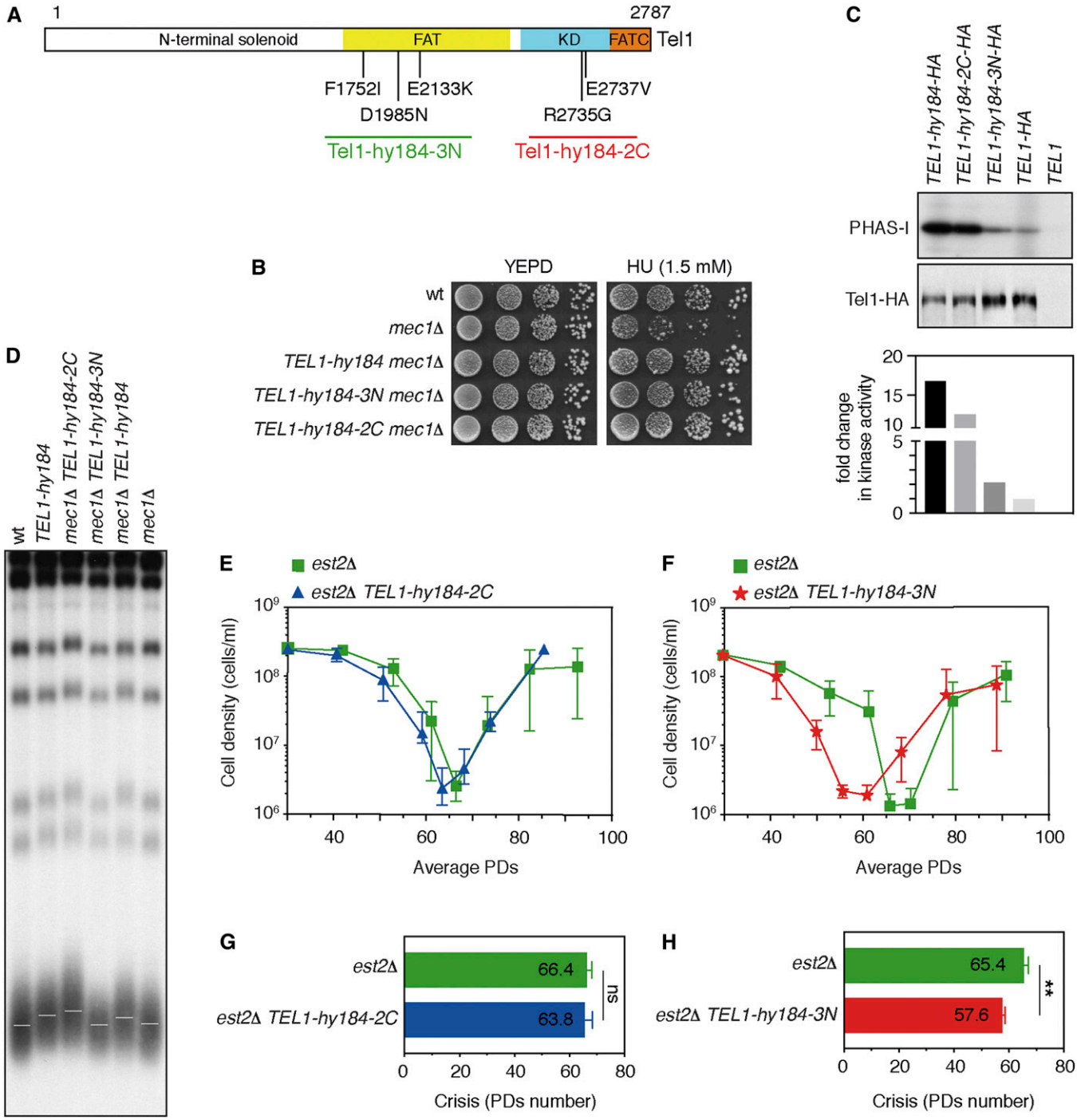

Figure 6 The F1752I, D1985N, and E2133K amino acidic substitutions promote anticipated senescence in telomerase-negative cells. (A) Schematic representation of the Tel1 protein with the position of the *TEL1–hy184* mutations. (B) Exponentially growing cell cultures were serially diluted (1:10) and each dilution was spotted out onto YEPD plates, with or without HU. (C) Protein extracts were immunoprecipitated with anti-HA antibodies, and subjected to a kinase assay on PHAS-I and γ-^{32}P-labeled ATP, before being analyzed by SDS-polyacrylamide gel electrophoresis. Immunoprecipitates were also subjected to western blot analysis with anti-HA antibodies. Band signals from kinase assays were normalized to band signals from western blots to determine the relative kinase activities. (D) *Xho*I-digested genomic DNA extracted from exponentially growing cell cultures was subjected to Southern blot analysis with a poly(GT) probe. (E–H) Senescence assays were performed as in Figure 1A. (E and F) The mean cell concentrations of independent spores with the same genotypes against PDs were plotted. Error bars denote SD. (G and H) The mean PD numbers at the peak of senescence (crisis) for each genotype are represented. Error bars denote SD. (E and G) *est2*Δ, $n = 8$; *est2*Δ *TEL1–hy184–2C*, $n = 12$. (F and H) *est2*Δ, $n = 6$; and *est2*Δ *TEL1–hy184–3N*, $n = 9$. Student's *t*-test: ** $P < 0.01$. FAT, FRAP–ATM–TRAPP; FATC, FAT C-terminal; KD, kinase domain; ns, not significant; PD, population doubling; wt, wild-type; YEPD, Yep medium supplemented with 2% glucose; HU, hydroxyurea.

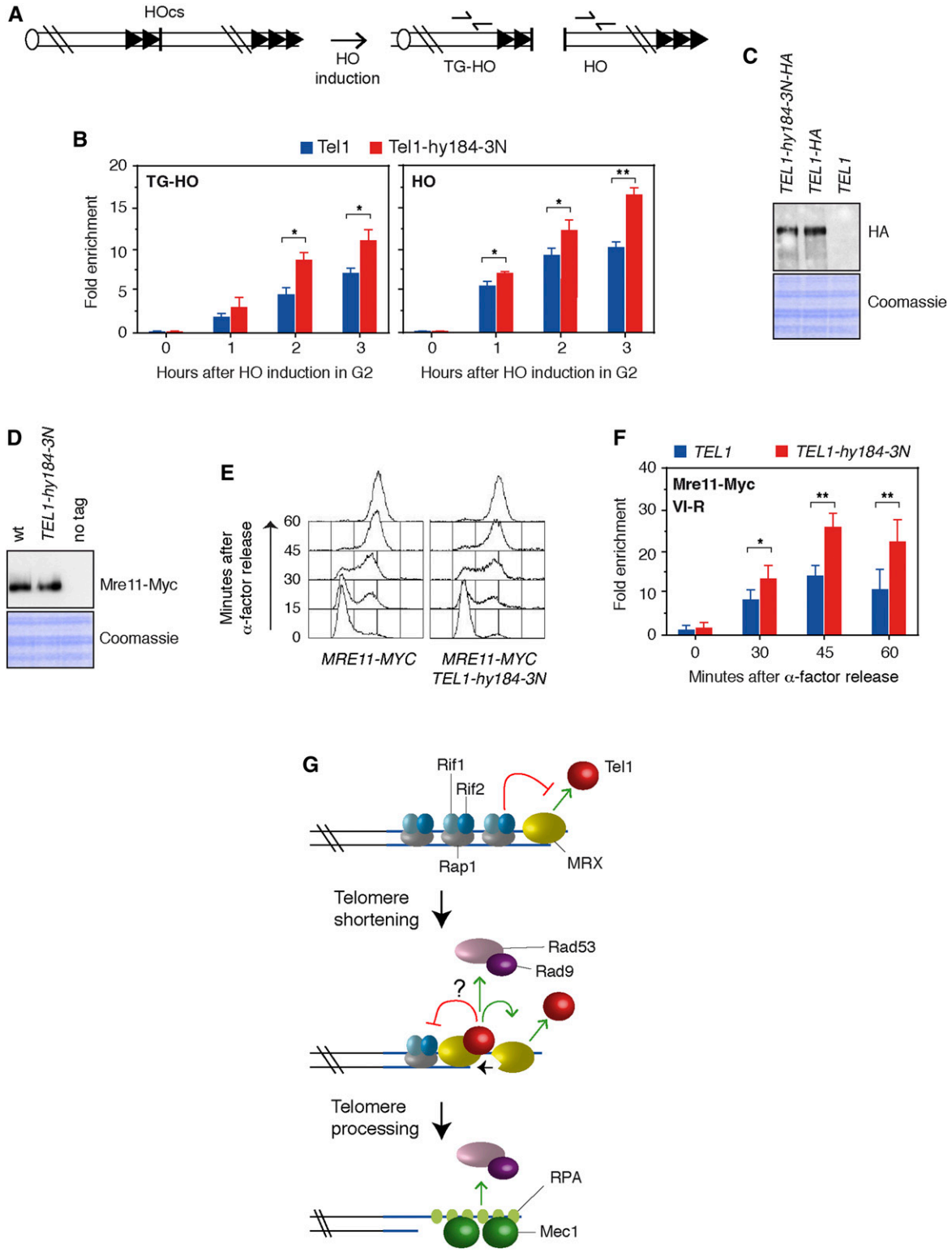

Figure 7 Recruitment of Tel1–hy184–3N to telomeres. (A) Schematic representation of the HO-induced telomere system. Primer pairs located 640 bp centromere-proximal to the HO cleavage site (TG–HO) and 550 bp centromere-distal to the HO cleavage site (HO), respectively, are indicated by arrows. (B) Chromatin samples prepared after HO induction to G2-arrested cells were immunoprecipitated with anti-HA antibodies and subjected to qPCR using primer pairs depicted in (A) and a primer pair located at the nontelomeric *ARO1* locus (CON). Data are expressed as relative fold enrichment of the TG–HO or HO signal over the CON signal after normalization to the input signals for each primer set. The data presented are means ± SDs from three different experiments. Student's *t*-test: * $P < 0.05$ and ** $P < 0.01$. (C and D) The same amounts of protein extracts from exponentially growing cells expressing HA-tagged Tel1 variants (C) or Myc-tagged Mre11 were subjected to western blotting with anti-HA or anti-Myc antibodies, respectively, or

hypermorphic *TEL1–hy184* allele, which was identified by its ability to compensate for Mec1 deficiency in response to DNA damage (Baldo *et al.* 2008), and the *tel1–kd* allele, which abolishes Tel1 kinase activity (Mallory and Petes 2000). Tel1–hy184 and Tel1–kd exert opposite effects on senescence kinetics: while Tel1–hy184 accelerates senescence in telomerase-negative cells, Tel1–kd delays it. Importantly, this effect on senescence is not due to a role of Tel1 in promoting ssDNA generation at DNA ends, as neither Tel1–hy184 nor Tel1–kd affect ssDNA generation at telomeres. Rather, the accelerated senescence caused by Tel1–hy184 in both wild-type and *MEC1*-deleted cells is completely dependent on Rad9, indicating that Tel1 plays a direct role in the induction of senescence independently of both ssDNA and Mec1.

However, the lack of Tel1, which reduces ssDNA at telomeres, appears to delay the onset of senescence slightly more severely than the absence of Tel1 kinase activity, which does not affect ssDNA generation. This result suggests that, although Tel1 induces replicative senescence mainly by directly signaling the presence of dysfunctional telomeres to the checkpoint, the function of Tel1 in telomere processing also contributes to senescence onset.

We show that Tel1 kinase activity is important to promote senescence independently of telomeric ssDNA generation, while the presence of Tel1, but not its kinase activity, is important to generate ssDNA at telomeres. These results extend previous findings indicating that Tel1 plays both kinase-dependent and -independent functions at telomeres, and that Tel1 kinase activity is essential for telomere elongation, while it is dispensable for the nucleolytic degradation of DSB ends (Greenwell *et al.* 1995; Mallory and Petes 2000; Baldo *et al.* 2008; Ma and Greider 2009; Martina *et al.* 2012; Gobbini *et al.* 2015; Cassani *et al.* 2016).

When we separated the two clusters of mutations present in the *TEL1–hy184* allele, we found that the R2735G and E2737V amino acid substitutions located in the kinase domain increased both kinase activity and telomere length, indicating a tight correlation between kinase activity and telomere length/telomerase activity, as previously observed (Greenwell *et al.* 1995; Mallory and Petes 2000; Baldo *et al.* 2008; Martina *et al.* 2012). However, these mutations do not significantly affect the onset of senescence in telomerase-negative cells. These findings indicate that, although Tel1 kinase activity is important to promote senescence, increased kinase activity alone is not sufficient to anticipate senescence. Interestingly, the F1752I, D1985N, and E2133K substitutions grouped in the FAT domain of Tel1 cause anticipated senescence in telomerase-negative cells, without affecting telomere length or Tel1 kinase activity. Furthermore, we show that *TEL1–hy184–3N* alleles enhance Tel1 and MRX binding at DNA ends. Therefore, more robust Tel1 binding at short telomeres appears to cause early senescence.

Tel1/ATM belongs to the phosphoinositide 3-kinase-related kinase (PIKK) family, a group of giant protein kinases that share some similarities in enzymatic activity, as well as common structures. All PIKKs have a conserved C-terminal kinase domain flanked by the conserved FAT and FAT C-terminal (FATC) domains, and an extensive helical solenoid N-terminal to the FAT domain (Figure 6A; Baretić and Williams 2014; Wang *et al.* 2016). Tel1/ATM is recruited to DNA ends through interaction with the C-terminal domain of the Xrs2/NBS1 subunit of the MRX/MRN complex (Nakada *et al.* 2003; Falck *et al.* 2005; You *et al.* 2005; Limbo *et al.* 2018). In *S. cerevisiae*, both the FATC domain and the N-terminal solenoid of Tel1 participate in the Tel1/Xrs2 interaction (Nakada *et al.* 2003; You *et al.* 2005; Ogi *et al.* 2015). However, the Tel1/MRX interaction appears to be more complex. In fact, Tel1/ATM interacts with a complex composed of only Mre11 and Rad50 (Lee and Paull 2004, 2005; Limbo *et al.* 2018). Furthermore, the characterization of separation-of-function *mre11* and *rad50* alleles, which specifically affect Tel1 activation, suggests that Tel1 interacts with Rad50 and Mre11 MRX subunits independently of Xrs2 (Cassani *et al.* 2019). Finally, each MRX subunit was found to interact with Tel1 in pull-down assays (Hailemariam *et al.* 2019).

Our results that the F1752I, D1985N, and E2133K substitutions in the FAT domain increase both Tel1 recruitment/persistence to DNA ends and Tel1 signaling in the absence of Mec1 suggest that the FAT domain controls Tel1 localization onto DNA, and that increased Tel1 association with eroded telomeres may be sufficient to generate a local Tel1-dependent checkpoint signal, which is then propagated through Rad9 and Rad53 (Figure 7G). As there is no evidence of a direct interaction between Tel1 and the DNA, and Tel1 appears to bind DNA only through MRX (Nakada *et al.* 2003; Falck *et al.* 2005; You *et al.* 2005; Limbo *et al.* 2018; Hailemariam *et al.* 2019), the FAT domain could mediate the interaction of Tel1 with MRX components or with proteins that modulate Tel1/MRX binding. Alternatively, the F1752I,

stained with Coomassie as a loading control. (E and F) Cells arrested in G1 with α-factor (αf) were released into the cell cycle. Cell samples taken at the indicated times after α-factor release were analyzed by FACS (E) or subjected to ChIP with anti-Myc antibodies (F). Co-immunoprecipitated DNA was analyzed by qPCR using primer pairs located at telomere VI-R and at the control *ARO1* locus (CON). The mean values ± SD are represented (n = 3). (F) Working model. The Rap1–Rif1–Rif2 complex inhibits MRX–Tel1 accumulation at telomeres, with Rif2 inhibiting MRX–Tel1 interaction. Telomere shortening in the absence of telomerase causes progressive loss of TG repeats and therefore of the negative control exerted by Rif2 on MRX–Tel1. As a consequence, MRX bound at short telomeres recruits Tel1, which in turn stimulates a further increase of both MRX and Tel1 to DNA possibly outcompeting with Rif2 for MRX binding. This local accumulation of Tel1 promotes activation of a Rad9- and Rad53-dependent checkpoint, and increases the amount of telomere-bound MRX, which contributes to generate ssDNA ends covered by Replication Protein A (RPA) that trigger Mec1 activation. ChIP, chromatin immunoprecipitation; HO, HOmothallic switching endonuclease; qPCR, quantitative PCR; ssDNA, single-stranded DNA; wt, wild-type.

D1985N, and E2133K substitutions might increase Tel1 signaling of eroded telomeres by modifying specific Tel1 interactions with substrates involved in checkpoint activation at telomeres but not in the control of ssDNA generation, and this enhanced checkpoint activation may in turn increase Tel1 localization at telomeres in a positive feedback loop.

Altogether, our results suggest that, as telomeres shorten in the absence of telomerase and the negative control exerted by Rif2 on MRX–Tel1 association to telomeres is progressively lost, MRX can bind short telomeres and recruits Tel1. Once recruited to telomeres, Tel1 possibly outcompetes with Rif2 for binding to MRX and stimulates a further increase of MRX, and therefore of Tel1 binding to DNA. This local accumulation of Tel1 promotes activation of a Rad9- and Rad53-dependent checkpoint, and concomitantly increases the amount of telomere-bound MRX, whose nucleolytic activity contributes to generate long ssDNA ends that trigger Mec1 activation (Figure 7G).

As the cellular response to short telomeres is now considered one of the most potent barriers to cancer emergence (Maciejowski and de Lange 2017), understanding how short telomeres trigger a crucial signal for the fate of cells and organisms is an important field in cancer research. Our findings that Tel1/ATM participates together with Mec1/ATR to activate a checkpoint response that promotes senescence in the presence of eroded telomeres contribute both to this field and to the elucidation of the multiple functions of Tel1/ATM at telomeres.

Acknowledgments

We thank D. Gottschling and R. Rothstein for providing yeast strains, J. Diffley for antibodies, G. Pietrapiana for preliminary results, and G. Lucchini and D. Bonetti for useful suggestions and critical reading of the manuscript. This work was supported by grants from Fondazione AIRC (Associazione Italiana per la Ricerca sul Cancro) under Investigator Grant IG 2017 (project identifier 19783) and the Progetti di Ricerca di Interesse Nazionale (2015) to M.P.L.

Literature Cited

Abdallah, P., P. Luciano, K. W. Runge, M. Lisby, V. Géli *et al.*, 2009 A two-step model for senescence triggered by a single critically short telomere. Nat. Cell Biol. 11: 988–993. [corrigenda: Nat. Cell Biol. 12: 520 (2010)]. https://doi.org/10.1038/ncb1911

Armstrong, C. A., and K. Tomita, 2017 Fundamental mechanisms of telomerase action in yeasts and mammals: understanding telomeres and telomerase in cancer cells. Open Biol. 7: 160338. https://doi.org/10.1098/rsob.160338

Arnerić, M., and J. Lingner, 2007 Tel1 kinase and subtelomere-bound Tbf1 mediate preferential elongation of short telomeres by telomerase in yeast. EMBO Rep. 8: 1080–1085. https://doi.org/10.1038/sj.embor.7401082

Baldo, V., V. Testoni, G. Lucchini, and M. P. Longhese, 2008 Dominant *TEL1-hy* mutations compensate for Mec1 lack of functions in the DNA damage response. Mol. Cell. Biol. 28: 358–375. https://doi.org/10.1128/MCB.01214-07

Ballew, B. J., and V. Lundblad, 2013 Multiple genetic pathways regulate replicative senescence in telomerase-deficient yeast. Aging Cell 12: 719–727. https://doi.org/10.1111/acel.12099

Baretić, D., and R. L. Williams, 2014 PIKKs--the solenoid nest where partners and kinases meet. Curr. Opin. Struct. Biol. 29: 134–142. https://doi.org/10.1016/j.sbi.2014.11.003

Bernstein, K. A., E. Shor, I. Sunjevaric, M. Fumasoni, R. C. Burgess *et al.*, 2009 Sgs1 function in the repair of DNA replication intermediates is separable from its role in homologous recombinational repair. EMBO J. 28: 915–925. https://doi.org/10.1038/emboj.2009.28

Bianchi, A., and D. Shore, 2007 Increased association of telomerase with short telomeres in yeast. Genes Dev. 21: 1726–1730. https://doi.org/10.1101/gad.438907

Bonetti, D., M. Clerici, S. Anbalagan, M. Martina, G. Lucchini *et al.*, 2010 Shelterin-like proteins and Yku inhibit nucleolytic processing of *Saccharomyces cerevisiae* telomeres. PLoS Genet. 6: e1000966. https://doi.org/10.1371/journal.pgen.1000966

Booth, C., E. Griffith, G. Brady, and D. Lydall, 2001 Quantitative amplification of single-stranded DNA (QAOS) demonstrates that cdc13-1 mutants generate ssDNA in a telomere to centromere direction. Nucleic Acids Res. 29: 4414–4422. https://doi.org/10.1093/nar/29.21.4414

Cassani, C., E. Gobbini, W. Wang, H. Niu, M. Clerici *et al.*, 2016 Tel1 and Rif2 regulate MRX functions in end-tethering and repair of DNA double-strand breaks. PLoS Biol. 14: e1002387. https://doi.org/10.1371/journal.pbio.1002387

Cassani, C., J. Vertemara, M. Bassani, A. Marsella, R. Tisi *et al.*, 2019 The ATP-bound conformation of the Mre11-Rad50 complex is essential for Tel1/ATM activation. Nucleic Acids Res. 47: 3550–3567. https://doi.org/10.1093/nar/gkz038

Chang, M., and R. Rothstein, 2011 Rif1/2 and Tel1 function in separate pathways during replicative senescence. Cell Cycle 10: 3798–3799. https://doi.org/10.4161/cc.10.21.18095

Clerici, M., V. Baldo, D. Mantiero, F. Lottersberger, G. Lucchini *et al.*, 2004 A Tel1/MRX-dependent checkpoint inhibits the metaphase-to-anaphase transition after UV irradiation in the absence of Mec1. Mol. Cell. Biol. 24: 10126–10144. https://doi.org/10.1128/MCB.24.23.10126-10144.2004

d'Adda di Fagagna, F., P. M. Reaper, L. Clay-Farrace, H. Fiegler, P. Carr *et al.*, 2003 A DNA damage checkpoint response in telomere-initiated senescence. Nature 426: 194–198. https://doi.org/10.1038/nature02118

D'Amours, D., and S. P. Jackson, 2001 The yeast Xrs2 complex functions in S phase checkpoint regulation. Genes Dev. 15: 2238–2249. https://doi.org/10.1101/gad.208701

de Lange, T., 2018 Shelterin-mediated telomere protection. Annu. Rev. Genet. 52: 223–247. https://doi.org/10.1146/annurev-genet-032918-021921

Dewar, J. M., and D. Lydall, 2010 Pif1- and Exo1-dependent nucleases coordinate checkpoint activation following telomere uncapping. EMBO J. 29: 4020–4034. https://doi.org/10.1038/emboj.2010.267

Diede, S. J., and D. E. Gottschling, 1999 Telomerase-mediated telomere addition *in vivo* requires DNA primase and DNA polymerases α and δ. Cell 99: 723–733. https://doi.org/10.1016/S0092-8674(00)81670-0

Dionne, I., and R. J. Wellinger, 1996 Cell cycle-regulated generation of single-stranded G-rich DNA in the absence of telomerase. Proc. Natl. Acad. Sci. USA 93: 13902–13907. https://doi.org/10.1073/pnas.93.24.13902

Enomoto, S., L. Glowczewski, and J. Berman, 2002 *MEC3*, *MEC1*, and *DDC2* are essential components of a telomere checkpoint pathway required for cell cycle arrest during senescence in *Saccharomyces cerevisiae*. Mol. Biol. Cell 13: 2626–2638. https://doi.org/10.1091/mbc.02-02-0012

Falck, J., J. Coates, and S. P. Jackson, 2005 Conserved modes of recruitment of ATM, ATR and DNA-PKcs to sites of DNA damage. Nature 434: 605–611. https://doi.org/10.1038/nature03442

Fallet, E., P. Jolivet, J. Soudet, M. Lisby, E. Gilson *et al.*, 2014 Length-dependent processing of telomeres in the absence of telomerase. Nucleic Acids Res. 42: 3648–3665. https://doi.org/10.1093/nar/gkt1328

Gao, H., T. B. Toro, M. Paschini, B. Braunstein–Ballew, R. B. Cervantes *et al.*, 2010 Telomerase recruitment in *Saccharomyces cerevisiae* is not dependent on Tel1-mediated phosphorylation of Cdc13. Genetics 186: 1147–1159. https://doi.org/10.1534/genetics.110.122044

Garvik, B., M. Carson, and L. Hartwell, 1995 Single-stranded DNA arising at telomeres in *cdc13* mutants may constitute a specific signal for the *RAD9* checkpoint. Mol. Cell. Biol. 15: 6128–6138. https://doi.org/10.1128/MCB.15.11.6128

Giraud–Panis, M. J., M. T. Teixeira, V. Géli, and E. Gilson, 2010 CST meets shelterin to keep telomeres in check. Mol. Cell 39: 665–676. https://doi.org/10.1016/j.molcel.2010.08.024

Gobbini, E., M. Villa, M. Gnugnoli, L. Menin, M. Clerici *et al.*, 2015 Sae2 function at DNA double-strand breaks is bypassed by dampening Tel1 or Rad53 activity. PLoS Genet. 11: e1005685. https://doi.org/10.1371/journal.pgen.1005685

Goudsouzian, L. K., C. T. Tuzon, and V. A. Zakian, 2006 *S. cerevisiae* Tel1p and Mre11p are required for normal levels of Est1p and Est2p telomere association. Mol. Cell 24: 603–610. https://doi.org/10.1016/j.molcel.2006.10.005

Grandin, N., A. Bailly, and M. Charbonneau, 2005 Activation of Mrc1, a mediator of the replication checkpoint, by telomere erosion. Biol. Cell 97: 799–814. https://doi.org/10.1042/BC20040526

Greenwell, P. W., S. L. Kronmal, S. E. Porter, J. Gassenhuber, B. Obermaier *et al.*, 1995 *TEL1*, a gene involved in controlling telomere length in *S. cerevisiae*, is homologous to the human ataxia telangiectasia gene. Cell 82: 823–829. https://doi.org/10.1016/0092-8674(95)90479-4

Grossi, S., A. Puglisi, P. V. Dmitriev, M. Lopes, and D. Shore, 2004 Pol12, the B subunit of DNA polymerase alpha, functions in both telomere capping and length regulation. Genes Dev. 18: 992–1006. https://doi.org/10.1101/gad.300004

Hailemariam, S., S. Kumar, and P. M. Burgers, 2019 Activation of Tel1^{ATM} kinase requires Rad50 ATPase and long nucleosome-free DNA but no DNA ends. J. Biol. Chem. 294: 10120–10130. https://doi.org/10.1074/jbc.RA119.008410

Hardy, J., D. Churikov, V. Géli, and M. N. Simon, 2014 Sgs1 and Sae2 promote telomere replication by limiting accumulation of ssDNA. Nat. Commun. 5: 5004. https://doi.org/10.1038/ncomms6004

Harley, C. B., B. Futcher, and C. W. Greider, 1990 Telomeres shorten during ageing of human fibroblasts. Nature 345: 458–460. https://doi.org/10.1038/345458a0

Hayflick, L., 1965 The limited *in vitro* lifetime of human diploid cell strains. Exp. Cell Res. 37: 614–636. https://doi.org/10.1016/0014-4827(65)90211-9

Hector, R. E., R. L. Shtofman, A. Ray, B. R. Chen, T. Nyun *et al.*, 2007 Tel1p preferentially associates with short telomeres to stimulate their elongation. Mol. Cell 27: 851–858. https://doi.org/10.1016/j.molcel.2007.08.007

Hirano, Y., K. Fukunaga, and K. Sugimoto, 2009 Rif1 and Rif2 inhibit localization of Tel1 to DNA ends. Mol. Cell 33: 312–322. https://doi.org/10.1016/j.molcel.2008.12.027

IJpma, A. S., and C. W. Greider, 2003 Short telomeres induce a DNA damage response in Saccharomyces cerevisiae. Mol. Biol. Cell 14: 987–1001. https://doi.org/10.1091/mbc.02-04-0057

Khadaroo, B., M. T. Teixeira, P. Luciano, N. Eckert–Boulet, S. M. Germann *et al.*, 2009 The DNA damage response at eroded telomeres and tethering to the nuclear pore complex. Nat. Cell Biol. 11: 980–987. https://doi.org/10.1038/ncb1910

Kim, N. W., M. A. Piatyszek, K. R. Prowse, C. B. Harley, M. D. West *et al.*, 1994 Specific association of human telomerase activity with immortal cells and cancer. Science 266: 2011–2015. https://doi.org/10.1126/science.7605428

Lee, J. H., and T. T. Paull, 2004 Direct activation of the ATM protein kinase by the Mre11/Rad50/Nbs1 complex. Science 304: 93–96. https://doi.org/10.1126/science.1091496

Lee, J. H., and T. T. Paull, 2005 ATM activation by DNA double-strand breaks through the Mre11-Rad50-Nbs1 complex. Science 308: 551–554. https://doi.org/10.1126/science.1108297

Limbo, O., Y. Yamada, and P. Russell, 2018 Mre11-Rad50-dependent activity of ATM/Tel1 at DNA breaks and telomeres in the absence of Nbs1. Mol. Biol. Cell 29: 1389–1399. https://doi.org/10.1091/mbc.E17-07-0470

Lundblad, V., and E. H. Blackburn, 1993 An alternative pathway for yeast telomere maintenance rescues *est1-* senescence. Cell 73: 347–360. https://doi.org/10.1016/0092-8674(93)90234-H

Lundblad, V., and J. W. Szostak, 1989 A mutant with a defect in telomere elongation leads to senescence in yeast. Cell 57: 633–643. https://doi.org/10.1016/0092-8674(89)90132-3

Ma, Y., and C. V. Greider, 2009 Kinase-independent functions of *TEL1* in telomere maintenance. Mol. Cell. Biol. 29: 5193–5202. https://doi.org/10.1128/MCB.01896-08

Maciejowski, J., and T. de Lange, 2017 Telomeres in cancer: tumour suppression and genome instability. Nat. Rev. Mol. Cell Biol. 18: 175–186. [corrigenda: Nat. Rev. Mol. Cell Biol. 20: 259 (2019)]. https://doi.org/10.1038/nrm.2016.171

Mallory, J. C., and T. D. Petes, 2000 Protein kinase activity of Tel1p and Mec1p, two *Saccharomyces cerevisiae* proteins related to the human ATM protein kinase. Proc. Natl. Acad. Sci. USA 97: 13749–13754. https://doi.org/10.1073/pnas.250475697

Mantiero, D., M. Clerici, G. Lucchini, and M. P. Longhese, 2007 Dual role for *Saccharomyces cerevisiae* Tel1 in the checkpoint response to double-strand breaks. EMBO Rep. 8: 380–387. https://doi.org/10.1038/sj.embor.7400911

Martina, M., M. Clerici, V. Baldo, D. Bonetti, G. Lucchini *et al.*, 2012 A balance between Tel1 and Rif2 activities regulates nucleolytic processing and elongation at telomeres. Mol. Cell. Biol. 32: 1604–1617. https://doi.org/10.1128/MCB.06547-11

Menin, L., S. Ursich, C. Trovesi, R. Zellweger, M. Lopes *et al.*, 2018 Tel1/ATM prevents degradation of replication forks that reverse after topoisomerase poisoning. EMBO Rep. 19: e45535. https://doi.org/10.15252/embr.201745535

Moriel-Carretero, M., P. Pasero, and B. Pardo, 2019 DDR Inc., one business, two associates. Curr. Genet. 65: 445–451. https://doi.org/10.1007/s00294-018-0908-7

Mozdy, A. D., and T. R. Cech, 2006 Low abundance of telomerase in yeast: implications for telomerase haploinsufficiency. RNA 12: 1721–1737. https://doi.org/10.1261/rna.134706

Nakada, D., K. Matsumoto, and K. Sugimoto, 2003 ATM-related Tel1 associates with double-strand breaks through an Xrs2-dependent mechanism. Genes Dev. 17: 1957–1962. https://doi.org/10.1101/gad.1099003

Ogi, H., G. H. Goto, A. Ghosh, S. Zencir, E. Henry *et al.*, 2015 Requirement of the FATC domain of protein kinase Tel1 for localization to DNA ends and target protein recognition. Mol. Biol. Cell 26: 3480–3488. https://doi.org/10.1091/mbc.E15-05-0259

Ritchie, K. B., and T. D. Petes, 2000 The Mre11p/Rad50p/Xrs2p complex and the Tel1p function in a single pathway for telomere maintenance in yeast. Genetics 155: 475–479.

Ritchie, K. B., J. C. Mallory, and T. D. Petes, 1999 Interactions of *TLC1* (which encodes the RNA subunit of telomerase), *TEL1*, and *MEC1* in regulating telomere length in the yeast *Saccharomyces cerevisiae*. Mol. Cell. Biol. 19: 6065–6075. https://doi.org/10.1128/MCB.19.9.6065

Sabourin, M., C. T. Tuzon, and V. A. Zakian, 2007 Telomerase and Tel1p preferentially associate with short telomeres in

S. cerevisiae. Mol. Cell 27: 550–561. https://doi.org/10.1016/j.molcel.2007.07.016

Shay, J. W., 2016 Role of telomeres and telomerase in aging and cancer. Cancer Discov. 6: 584–593. https://doi.org/10.1158/2159-8290.CD-16-0062

Shiloh, Y., and Y. Ziv, 2013 The ATM protein kinase: regulating the cellular response to genotoxic stress, and more. Nat. Rev. Mol. Cell Biol. 14: 197–210. https://doi.org/10.1038/nrm3546

Stewart, S. A., and R. A. Weinberg, 2006 Telomeres: cancer to human aging. Annu. Rev. Cell Dev. Biol. 22: 531–557. https://doi.org/10.1146/annurev.cellbio.22.010305.104518

Takata, H., Y. Kanoh, N. Gunge, K. Shirahige, and A. Matsuura, 2004 Reciprocal association of the budding yeast ATM-related proteins Tel1 and Mec1 with telomeres *in vivo*. Mol. Cell 14: 515–522. https://doi.org/10.1016/S1097-2765(04)00262-X

Teixeira, M. T., 2013 *Saccharomyces cerevisiae* as a model to study replicative senescence triggered by telomere shortening. Front. Oncol. 3: 101. https://doi.org/10.3389/fonc.2013.00101

Teixeira, M. T., M. Arneric, P. Sperisen, and J. Lingner, 2004 Telomere length homeostasis is achieved via a switch between telomerase-extendible and -nonextendible states. Cell 117: 323–335. https://doi.org/10.1016/S0092-8674(04)00334-4

Tsukamoto, Y., A. K. Taggart, and V. A. Zakian, 2001 The role of the Mre11-Rad50-Xrs2 complex in telomerase- mediated lengthening of *Saccharomyces cerevisiae* telomeres. Curr. Biol. 11: 1328–1335. https://doi.org/10.1016/S0960-9822(01)00372-4

Vasianovich, Y., and R. J. Wellinger, 2017 Life and death of yeast telomerase RNA. J. Mol. Biol. 429: 3242–3254. https://doi.org/10.1016/j.jmb.2017.01.013

Villa, M., C. Cassani, E. Gobbini, D. Bonetti, and M. P. Longhese, 2016 Coupling end resection with the checkpoint response at DNA double-strand breaks. Cell. Mol. Life Sci. 73: 3655–3663. https://doi.org/10.1007/s00018-016-2262-6

Vodenicharov, M. D., and R. J. Wellinger, 2006 DNA degradation at unprotected telomeres in yeast is regulated by the CDK1 (Cdc28/Clb) cell-cycle kinase. Mol. Cell 24: 127–137. https://doi.org/10.1016/j.molcel.2006.07.035

Wang, X., H. Chu, M. Lv, Z. Zhang, S. Qiu *et al*., 2016 Structure of the intact ATM/Tel1 kinase. Nat. Commun. 7: 11655. https://doi.org/10.1038/ncomms11655

Wellinger, R. J., and V. A. Zakian, 2012 Everything you ever wanted to know about *Saccharomyces cerevisiae* telomeres: beginning to end. Genetics 191: 1073–1105. https://doi.org/10.1534/genetics.111.137851

Wellinger, R. J., K. Ethier, P. Labrecque, and V. A. Zakian, 1996 Evidence for a new step in telomere maintenance. Cell 85: 423–433. https://doi.org/10.1016/S0092-8674(00)81120-4

You, Z., C. Chahwan, J. Bailis, T. Hunter, and P. Russell, 2005 ATM activation and its recruitment to damaged DNA require binding to the C terminus of Nbs1. Mol. Cell. Biol. 25: 5363–5379. https://doi.org/10.1128/MCB.25.13.5363-5379.2005

Zubko, M. K., L. Maringele, S. S. Foster, and D. Lydall, 2006 Detecting repair intermediates *in vivo*: effects of DNA damage response genes on single-stranded DNA accumulation at uncapped telomeres in budding yeast. Methods Enzymol. 409: 285–300. https://doi.org/10.1016/S0076-6879(05)09016-6

Communicating editor: J. Surtees